IAC-02-J.6/T.5.02

Initial Characterization of the Microgravity Environment of the International Space Station: Increments 2 Through 4

Kenol Jules, Kevin McPherson
NASA Glenn Research Center, Mail Stop 77-7, 21000 Brookpark Rd., Cleveland, OH 44135-3191, USA

Kenneth Hrovat, Eric Kelly
ZIN Technologies, Inc., MS 77-7, 21000 Brookpark Rd., Cleveland, OH 44135-3191, USA

Abstract

The primary objective of the International Space Station is to provide a long-term quiescent environment for the conduct of scientific research for a variety of microgravity science disciplines.
This paper reports to the microgravity scientific community the results of an initial characterization of the microgravity environment on the International Space Station for increments 2 through 4. During that period almost 70,000 hours of station operations and scientific experiments were conducted. 720 hours of crew research time were logged aboard the orbiting laboratory and over half a terabyte of acceleration data was recorded and much of that was analyzed. The results discussed in this paper cover both the quasi-steady and vibratory acceleration environment of the station during its first year of scientific operation.

For the quasi-steady environment, results are presented and discussed for the following: the space station attitudes Torque Equilibrium Attitude and the X-Axis Perpendicular to the Orbital Plane; station docking attitude maneuvers; Space Shuttle joint operation with the station; cabin de-pressurizations and the station water dumps.

For the vibratory environment, results are presented for the following: crew exercise, docking events, and the activation/de-activation of both station life support system hardware and experiment hardware. Finally, a grand summary of all the data collected aboard the station during the one-year period is presented showing where the overall quasi-steady and vibratory acceleration magnitude levels fall over that period of time using a 95^{th} percentile benchmark.

1 Introduction

The International Space Station (ISS) orbits Earth, traveling at 17,500 mph, providing a unique laboratory where engineers and scientists can challenge their abilities and imaginations to advance science and technology. During the first year of continuous human presence aboard ISS, almost 70,000 hours of station operations and scientific experiments were conducted, with investigations controlled by astronauts in space and remotely by scientists on the ground [1].

A major purpose of the station is to provide a low-gravity environment for fundamental science and commercial research. To ascertain that such goal is met, two accelerometer systems were flown to ISS to continuously measure the environment. These two accelerometers are sponsored by the NASA Office of Biological and Physical Research (OBPR), which sponsors science experiments on various low gravity carriers/platforms and facilities such as the STS, Keplerian flight-path aircraft, sounding rockets, drop towers and, of course, the ISS.

With the completion of the flight of Space Transportation System (STS)-100 (flight 6A), the Microgravity Environment Program (MEP) at the National Aeronautics Space Administration (NASA) Glenn Research Center (GRC) delivered two acceleration measurement systems to the International Space Station (ISS). These acceleration measurement systems provide a generic service to microgravity payloads by measuring the quasi-steady and vibratory acceleration environments on board the station. The Microgravity Acceleration Measurement System (MAMS) measures accelerations in the quasi-steady regime, including the contributions of aerodynamic drag, vehicle rotation, and vehicle venting effects. The Space Acceleration Measurement System (SAMS) measures on-board disturbances in the vibratory regime resulting from vehicle systems, crew activity, and experiment hardware.

The two accelerometer systems provide support to experiments requiring acceleration measurements in the vibratory as well as the quasi-steady regimes. The two accelerometer systems were deployed to the ISS on April 19, 2001. The SAMS team and the Principal Investigator Microgravity Services (PIMS) project at

the NASA-GRC, Cleveland, Ohio, are attending to these two accelerometers.

The NASA GRC PIMS project has the responsibility for processing and archiving acceleration measurements, analyzing these measurements, characterizing the reduced gravity environment in which the measurements were taken, and providing expertise in low gravity environment assessment for a variety of carriers/platforms and facilities, such as the STS, Keplerian flight-path aircraft, sounding rockets, drop towers and the ISS in support of the NASA's Physical Science Division Principal Investigators (PIs). The PIMS project supports PIs from the microgravity science disciplines of biotechnology, combustion science, fluid physics, material science, fundamental physics and the astronaut training office. The PIMS project is funded by the NASA Headquarters and is part of the NASA GRC's MEP, which integrates the analysis and interpretation component of PIMS with the various NASA sponsored acceleration measurement systems. The PIMS project is responsible for receiving, processing, analyzing, displaying, distributing and archiving the acceleration data for SAMS and MAMS during their operation aboard the ISS. This paper discusses the results of measurements taken by these two systems during their first year of operation aboard the ISS. The discussion in this paper covers the period of May 2001 to May 2002.

2 Microgravity Environment

The microgravity acceleration environment of an orbiting spacecraft in low earth orbit is a complex phenomenon. Many factors [2], such as experiment operation, life-support systems, equipment operation, crew activities, aerodynamic drag, gravity gradient, rotational effects as well as the vehicle structural resonance frequencies (structural modes) contribute to form the overall microgravity environment. For ease of analysis, the microgravity acceleration environment can be considered as made up of three components: quasi-steady, vibratory, and transient components.

2.1 Quasi-steady

The quasi-steady component [3] is composed of those accelerations whose frequency is less than the lowest natural structural frequency of the vehicle. Those accelerations vary over long periods of time, typically longer than a minute. This lowest natural structural frequency depends on the vehicle. For the ISS, the lowest natural structural frequency [4] is expected to be around 0.1 Hz. The system configuration and mass properties, the specified altitude, and the attitude control system are the principal contributors [5] to the quasi-steady accelerations for the ISS.

2.2 Vibratory

The vibratory component is composed of those accelerations, which are oscillatory in nature and whose frequencies are greater than or equal to the lowest natural structural frequency of the vehicle. They are harmonic and periodic in nature with a characteristic frequency. For the ISS, the characteristic frequencies [5] of disturbance are expected to be in the range of sub-Hertz to hundreds of Hertz (0.01 – 300 Hz). The vibratory component includes accelerations caused by equipment operation such as pumps, fans, communication antenna dither motion, centrifuges, compressors, crew activity, exercise, and structural mode excitations.

2.3 Transient

The transient component is composed of those accelerations that last for a short periods of time, and are non-repetitive. The transient component [5] includes accelerations caused by the ISS thruster operations, experiment operations, docking and undocking, Intra-Vehicular Activity (IVA), Extra-Vehicular Activity (EVA), and crew actions.

3 Accelerometers

One of the major goals of the ISS is to provide a quiescent reduced gravity environment to perform fundamental scientific research. However, small disturbances aboard the ISS impact the overall environment. Such small disturbances need to be measured in order to assess their potential impact on the science. In order to provide support for the science, which requires acceleration data measurement on the ISS, SAMS and MAMS were installed on the ISS. MAMS started taking measurements on the ISS on May 3rd, 2001, while SAMS started on June 4th, 2001. SAMS can measure vibratory acceleration data in the range of 0.01 to 400 Hz for payloads requiring such measurements [6]. MAMS consists of two sensors. 1) MAMS Orbital Acceleration Research Experiment (OARE) Sensor Subsystem (OSS), MAMS-OSS, a low frequency range sensor (DC to 1 Hz), is used to characterize the quasi-steady environment for payloads and the ISS vehicle. 2) MAMS-High Resolution Accelerometer Package (HiRAP) is used to characterize the ISS vibratory environment up to 100 Hz [7].

4 ISS Increment 2 to 4 Configurations

The ISS is a global partnership of many nations. This project is an engineering, scientific, and technological quantum leap ushering in a new era of human space exploration. Assembly of the ISS began in late 1998 [8] and will continue until completion sometime around the year 2004. During its assembly and over its nominal 10-year lifetime, the ISS will serve as an orbital platform for the United States and its International partners to make advances in life sciences, microgravity sciences, space sciences, earth sciences, commercial product development and engineering research and technology.

This paper focuses on Increments 2 to 4 (from May 2001 to May 2002) and not on ISS at assembly complete. An Increment duration averages about 4 months (sometimes more) and is determined by crew rotations and flights to/from ISS**.** Table 1 shows all the major missions/flights (no Progress flights and Soyuz taxi vehicles are shown) to ISS during the period covered by Increments 2 to 4. Each increment has a theme that focuses on the primary science or activities to be performed. Increment-2's theme was radiation; Increment-3 was bone and muscle research and Increment-4 was plants in space. Increment-2 began with the following modules on-orbit: Unity (Node), Zarya (Functional Cargo Block), Zvezda (Service Module) and Destiny. In April 2001, the Canadarm2 was installed to ISS. The last item that was added during Increment-2 to the ISS was the Quest Airlock to the Unity Node in July 2001. The Russian Docking Compartment (DC-1), Pirs, and the Strela Boom were added to ISS in September 2001 during Increment-3. The Pirs module serves as an additional docking port for visiting Soyuz and Progress craft, and as an airlock from which Russian segment spacewalks can be conducted. The station grew again during Increment-4 with the addition of the S0 (S-zero) Truss in April 2002 and the addition of the Mobile Base System (MBS) in June 2002**.** Figure 1 shows the evolution of the station from Increment-2 to 4.

5 Data Measurement Aboard the ISS

During Increments-2 to 4, five SAMS Sensor Enclosure (SE) heads were activated: 121F02 through 121F06. Each sensor head had a defined coordinate system whose location and orientation is defined with respect to the Space Station Analysis Coordinate System [9-12], Table 2. Each origin is defined as the triaxial center point of the three accelerometers that comprise the head. SAMS SE 121F02 was mounted in the SAMS International Subrack Interface Standard (ISIS) drawer 1 in the Expedite the Processing of Experiments of the Space Station (EXPRESS) Rack 1. EXPRESS Rack 1 was located in the overhead bay 2 of the US Laboratory Module (LAB1O2). Head 121F03 was mounted on the lower Z panel assembly below EXPRESS Rack 2. EXPRESS Rack 2 was located in overhead bay 1 of the US laboratory Module (LAB1O1). Head 121F04 was mounted on the lower Z panel assembly below EXPRESS Rack 1; head 121F05 was mounted on the bracket around the upper Z panel light assembly of EXPRESS Rack 2; and head 121F06 was mounted on the front panel of EXPRESS Rack 2 in support of the Experiment of Physics of Colloids in Space (EXPPCS). Figure 2, and Table 3 show the location of each SAMS SE heads on each EXPRESS Rack and their distance relative to each other.

During Increments 2 to 4, MAMS was located in the middeck lockers 3 and 4 of EXPRESS Rack 1. The origin of the OSS coordinate system is located at the center of gravity of the OSS proof mass. Table 2 shows the location of the OSS and HiRAP with respect to the ISS coordinate system and Figures 2 and 3 show the location and distance of MAMS in EXPRESS Rack 1 relative to the SAMS SEs.

Tables 2 and 3 show the precise location of each SAMS SE and MAMS-OSS/HiRAP sensors within the US LAB and their distance from each other in each rack as well as rack locations relative to each other. Table 3 shows the distance, in inches, each sensor is mounted from the other in the US LAB coordinate system. Figure 4 shows the US LAB dimension, coordinate system as well as the ISS-United States Orbital Segment (USOS) analysis coordinate system. (Please note that the USOS analysis coordinate system is different from the Russian Orbital Segment (ROS) analysis coordinate system (see Figure 5)) Table 3 shows the distance between each sensor in magnitude level while Table 2 shows the same information, but in both the US LAB and ISS-USOS coordinate systems as well as the distance from the US LAB forward hatch (see Figure 4) and the delta from the geometric center of EXPRESS Racks 1 and 2 to each of the sensors. These two Tables along with Figure 4 provide a clear picture of the exact location of each sensor and Racks 1 and 2 inside the US LAB.

From May 2001 to May 2002 (the span covered in this paper), the five SAMS SE heads and MAMS-0SS and MAMS-HiRAP have recorded over half a terabyte of acceleration data from the ISS, approaching about 50,000 hours (for all the sensors combined). Table 4 shows how much acceleration data the PIMS project has archived for each sensor head on a monthly basis.

In Table 4, ossbtmf stands for Trimmed Mean Filter (TMF) acceleration data from MAMS-OSS, while ossraw stands for acceleration data that has not been trimmed mean filtered (i.e., raw data).

6 Data Analysis Techniques and Processing

Due to limitations of the accelerometer systems, namely SAMS for this discussion, it is standard practice to demean vibratory data. Focus is instead placed on the dynamic, oscillatory components of the acceleration environment. Specialized measurement systems and procedures are used to collect and analyze the quasi-steady components of acceleration.

The basis for the frequency domain analyses that were performed is the acceleration power spectral density (PSD). The PSD is a function that quantifies the distribution of power in a signal with respect to frequency. When properly applied, it serves as a powerful tool to help identify and quantify oscillatory components of the acceleration environment. An introductory presentation of the PSD along with other vibratory analysis techniques is given in [13]. Mathematical foundation and important details are given in [14,15].

Displays of acceleration PSDs can give much useful information, but keen insight to the dynamic nature of the acceleration spectrum aboard a manned spacecraft comes when numerous PSDs are arrayed as a function of time or combined in the form of a two-dimensional histogram. A spectrogram is a three-dimensional plot that shows PSD magnitude (represented by color) versus frequency versus time. It is a powerful qualitative tool for characterizing long periods of data. Boundaries and structure in both time and frequency become apparent with this type of display. When acceleration PSDs are laid out versus time for regular 8-hour intervals, the resulting displays are referred to as roadmap spectrograms or simply roadmaps. Alternatively, rather than show PSDs versus time, they can be combined in the form of a two-dimensional histogram as discussed in [13]. A display of acceleration spectra in this form is referred to here as a Principal Component Spectral Analysis (PCSA) plot. Its name stems from the fact that it serves to summarize magnitude and frequency variations of key spectral contributors for a relatively long period of time.

The basis for the amplitude domain analyses that were performed for the vibratory data is the acceleration magnitude histogram. Simply stated, the vector magnitude for each of the orthogonal acceleration record (XYZ) triplets was calculated and the resulting array of acceleration magnitudes is then input to a routine that counts the number of occurrences for each of several equally spaced acceleration magnitude bins. This gives the acceleration magnitude histogram. The cumulative percentage of occurrence as a function of acceleration magnitude can then be computed to yield percentile values.

Amplitude domain information does not give the insight that can be gleaned from acceleration spectrograms, but histograms computed on an hourly basis and then selectively combined (summed) can give a simple measure of "near worst case" conditions. The measure that was used here is an approximate 95th percentile extraction from the cumulative percentage of occurrence for the combined histogram.

7 ISS Quasi-steady Microgravity Environment Characterization

The quasi-steady regime is comprised of accelerations with frequency content below 0.01 Hz and magnitudes expected to be on the order of 2 μg or less. These low-frequency accelerations are associated with phenomena related to the orbital rate, primarily aerodynamic drag. However, gravity gradient and rotational effects may dominate in this regime, depending on various conditions and an experiment's location relative to the vehicle's center of mass (CM). Another source of acceleration considered in this regime is venting of air and / or water from the station. This event results in a nearly constant, low-level propulsive force. The different quasi-steady environment characteristics seen on the ISS during the period covered by this paper are mainly due to altitude and attitude of the station. Variation in atmospheric density with time and altitude contribute to the differences in the aerodynamic drag component. Different attitudes will affect the drag component due to the variation of the frontal cross-sectional area of the station with respect to the velocity vector (direction of flight).

7.1 Attitude Effects

7.1.1 Torque Equilibrium Attitude (TEA)

Torque Equilibrium Attitude (TEA) is an attitude that balances the vehicle's gravity gradient and aerodynamic drag torques. This is the attitude that will be flown during microgravity mode to support scientific research at assembly complete. However, TEA will vary with station configuration because of change in mass and

aerodynamic properties. During Increments 2, 3 and 4, the nominal TEA attitude was near Yaw, Pitch, Roll (YPR) = (350, 350, 0) relative to the Local Vertical Local Horizontal (LVLH) coordinate system. Figure 1 shows the acceleration vs. time plot of MAMS OSS data, collected during Increment-4 at GMT 133/22:30. For the 8 hour time period covered in Figure 6, the crew was asleep and the ISS was in TEA.

7.1.2 X-Principal Axis Perpendicular to the Orbit Plane (XPOP)

X Principal Axis Perpendicular to the Orbit Plane (XPOP) is a sun-tracking, quasi-inertial flight attitude used for power generation. In this attitude, the vehicle's X_A axis is maintained perpendicular to the direction of flight, while the Y_A and Z_A axes are alternately subjected to the drag and gravity gradient vectors as the vehicle completes an orbit. The cyclical profiles generated in the Y_A and Z_A axes are very pronounced in the time series plot in Figure 7. The relatively constant 1.82 μg offset in the X_A axis is the gravity gradient effect due to the distance of the OSS sensor from the center of mass of the vehicle in the X_A direction.

7.2 Docking/Undocking

In terms of the quasi-steady environment, the impact of the physical mating/unmating of the two vehicles during a docking/undocking event is less of a disturbance than the attitude adjustments in preparation for the event. Figure 8 shows the first undocking event captured in MAMS-OSS data, which was the Soyuz TM-31 undocking at GMT 126/02:20:49. At GMT 126/00:19:58, the station began an attitude maneuver to change from +XVV/+ZLV (X_A-axis in the direction of the velocity vector, Z_A–axis towards nadir) to -XVV/+ZLV (X_A-axis opposite the velocity vector), which was a yaw of 180 degrees about the Z_A axis. Two hours later, after the Soyuz undocked, the ISS returned to its original attitude. Both maneuvers are seen as offsets between 10-25 μg in the X_A axis, and to a lesser extent in the Y_A and Z_A-axes.

7.3 Venting and Water Dump

Venting of gas and water to space produce a low level propulsive force, which affects the quasi-steady regime. Figure 9 shows the quasi-steady effects of a condensate water dump that occurred during Increment-4, beginning at GMT 012/15:30 and ending at GMT 012/16:50. The ISS was directed to an attitude, YPR= (273.3, 356.7, 307.0), that placed the vent in retrograde to minimize contamination. The effects of the attitude maneuvers are out of the time range of this plot. The major disturbance occurs in the Z_A-axis, peaking in magnitude at approximately -6 μg at the 0.8-hour mark.

7.4 Depressurization

During Increment-3, a new docking compartment, DC-1, docked to the nadir port on the Service Module. Depressurization of the DC-1 volume occurs prior to Russian-based Extra-Vehicular Activities (EVAs). One such event began at GMT 316/02:35. Figure 10 shows the effect of the depressurization event on the quasi-steady environment. The dotted box highlights the depressurization with steps of -6 μg, -2 μg and -4 μg in the X_A, Y_A and Z_A-axes respectively.

Table 5 gives a summary of events measured by MAMS OSS sensor during increments 2-4. For more information on each of these events see [10-12].

8 ISS Vibratory Microgravity Environment Characterization

The vibratory acceleration regime consists of the acceleration spectrum from 0.01 to 300 Hz, with magnitudes expected to vary greatly depending on the nature of the disturbance and on the transmissibility from the source to the location of interest. The relatively high frequency accelerations that shape the vibratory environment of the ISS are usually associated with vehicle operations, vehicle systems, experiment-related equipment, and crew activity. This section examines the effects of some of these vibratory disturbances as measured by SAMS sensors.

8.1 Crew Exercise

Based on a large volume of acceleration data from various Shuttle microgravity missions, experience has shown that individual crew vigor is a fundamental factor on the impact of ergometer exercise. Naturally, the more vigorous the individual exercised, the more pronounced was the impact. It is not the intent here to track how energetic various crew are during exercise, but consideration of this factor may prove useful at some point in the future.

8.1.1 Treadmill Vibration Isolation System

Based on numerous reported Treadmill Vibration Isolation System (TVIS) exercise periods, no clear

signature is evident from the Russian Service Module (SM) TVIS in the US Lab SAMS measurements.

8.1.2 Cycle Ergometer With Vibration Isolation System

Proximity of the Cycle Ergometer with Vibration Isolation System (CEVIS), in the US Lab Port side, Bay 3 (LAB1P3) to ER1, in the US Lab Overhead, Bay 2 (LAB1O2) and ER2, in Overhead, Bay 1(LAB1O1) makes it a candidate for propagating oscillatory disturbances from its mounting location to the vibratory sensors in the nearby EXPRESS racks. Two time spans that include CEVIS exercise were analyzed to characterize the measured effects at various accelerometer locations. These particular periods were considered for two reasons. They both: (1) exhibit ergometer acceleration signature based on experience from Shuttle ergometer exercise, and (2) correlate well with exercise data collected independently of the accelerometers. The correlating data came in the form of spreadsheet files recorded on PCMCIA cards aboard TVIS and CEVIS with all personal or sensitive information filtered out on the ground at the Johnson Space Center (JSC).

For the first exercise period analyzed, the spectrogram in Figure 11 clearly shows an ergometer signature (as marked near bottom right), starting just before Greenwich Mean Time (GMT) 01-January-2002, 001/11:13:34. The spectrogram's end time truncates the exercise period because this time marks the beginning of a PIMS Archived Data (PAD) gap. The narrowband peak at about 2.5 Hz marked on the lower right of the spectrogram is the pedaling frequency. For Shuttle ergometer exercise, the pedaling signature was accompanied by that of shoulder sway with frequency around half the pedal rate. On the ISS, for this CEVIS exercise period, the shoulder sway signature is obscured by structural modes that fall in the same frequency range. To quantify the impact of this exercise period from this and other sensor locations, the cumulative Root Mean Square (RMS) acceleration versus frequency curves of Figure 12 were computed. The curves in this figure all step up about 70 μg_{RMS} at the pedaling frequency, but vary to some degree across the rest of the acceleration spectrum below 10 Hz. The variability is expected as the SAMS sensors used for the analysis were distributed throughout ER1 and ER2 as indicated by the legend.

A second, much quieter, CEVIS exercise period was analyzed for data collected on GMT 03-January-2002. Only minimal impact was registered at the pedaling frequency near 2.8 Hz.

8.1.3 Russian Velosiped Ergometer (Velo)

Close look at roadmap spectrograms for GMT 25-July-2002 to 31-July-2002 shows what is most certainly the signature of daily Velo exercise for a couple of hours around GMT 18:00 (see below 5 Hz on Figure 13). An in-depth quantification for the pedal rate peak can be seen in the 8-second interval RMS acceleration plot of Figure 14. The RMS acceleration was computed for the frequency range from 2.1 to 2.3 Hz. To the right of the 12:00 time tick, just before 13:00, there is a 10-minute exercise period. This shows a step up from a baseline of about 2 μg_{RMS} without Velo to between 50 and 100 μg_{RMS} when the Velo is being used. This step up from baseline occurs again around the 18:00 mark (as mentioned above).

Similar analyses were performed for another Velo exercise period for data collected around GMT 06-August-2002, 218/17:00:00. For the active SAMS sensor locations, the sub 5 Hz RMS level was well below 100 μg_{RMS} when no Velo exercise was taking place around that time, but often was in excess of 150 μg_{RMS} during this exercise period.

8.2 Vehicle Operations

This section covers some of the ISS operations, which affects the overall microgravity environment. The following activities are reviewed: the Russian Progress reboost of ISS, the Progress vehicle docked with ISS, the US Space Shuttle docked to as well as joint operation with ISS, and the Russian SKV air conditioner compressor.

8.2.1 Progress Reboost

To assess the impact of burns for reboost 3 and reboost 4 cited in the Table 6, consider an hour period around the times shown in the first 2 rows of Table 6. Considering the 1-hour period starting at GMT 06-March-2002, 065/03:08:30 for reboost 3, we see a noticeable upward step of the acceleration vector magnitude in Figure 15 around the 30-minute mark. The timestamps affiliated with the acceleration measurements indicate the reboost 3 burn went from GMT 06-March-2002, 065/03:37:23 to 03:40:03. If we consider the same spans for SAMS sensor 121F02 and 121F04, then we can compare the median acceleration vector magnitudes for times before/after the burn to

those during the burn and get the results shown in Table 7.

Note that in each case, the median acceleration vector magnitudes were over 700 µg during the Progress reboost burn and the largest difference was seen in the 121F03 data for reboost 3.

8.2.2 Progress, Flight 4P

A Russian Progress vehicle docked with the ISS at GMT 23-May-2001 00:24. The cargo vehicle docked at the aft docking port of the Service Module. This docking event was registered as a 10 mg impulse by the MAMS HiRAP at GMT 23-May-2001 00:24:20. This transient was followed a few seconds later by a slightly larger, 13 mg peak, which occurred at about GMT 23-May-2001 00:24:23.

8.2.3 Space Shuttle Atlantis (STS-104), Flight 7A Docking

The Space Shuttle Atlantis docked with the ISS at GMT 14-July-2001 03:08 to begin Flight 7A joint operations. This was evidenced in the HiRAP spectrogram of Figure 16, which shows initial contact or softmate as a vertical (red) streak just before the 30-minute mark. A peak acceleration magnitude of just over 10 mg was recorded by HiRAP at GMT 14-July-2001 03:08:31, while a peak acceleration magnitude of a little more than 6 mg at GMT 14-July-2001 03:21:04 was registered. This was the time of the final mechanical capture or hardmate as seen starting at this time in Figure 16. This coupling introduces a structural path for transmission of the Shuttle's Ku-band antenna 17 Hz dither.

The Ku-band antenna is dithered to avoid mechanical stiction while tracking communications satellites, and is mounted on the Shuttle's forward, starboard cargo bay sill. Meanwhile, the measurements used to compute the aforementioned spectrogram were collected at the MAMS HiRAP location in EXPRESS Rack 1 of the US Lab. As a means of quantifying transmission of this 17 Hz disturbance from the Shuttle to the ISS, Parseval's theorem was employed to compute cumulative RMS acceleration versus frequency curves. For reference, SAMS on Shuttle during past microgravity missions routinely registered the dither disturbance between just below 100 μg_{RMS} and up to around 300 μg_{RMS} [16]. For the Atlantis 7A docking, the HiRAP sensor registered the tightly controlled disturbance shown in Table 8.

After more than 8 days of Flight 7A joint operations, Figure 17 shows that the Space Shuttle Atlantis undocked from the ISS at GMT 22-July-2001 04:54. This is evidenced by the sudden disappearance of the Shuttle's Ku-band antenna 17 Hz dither signature at just after the 30-minute mark of the spectrogram. Vehicle separation was initiated by means of four spring-loaded pushers [17]. Notable peak accelerations measured by HiRAP during undocking time are shown in Table 9.

8.2.4 SKV Air Conditioner

Part of the Environmental Control and Life Support System (ECLSS) is located in the Service Module (SM), this vehicle subsystem introduces a narrowband disturbance at about 23.5 Hz. There are occasions when one, both, or neither of the 2 SKVs are operating, but nominally, one is normally on. Early characterization and analysis of SKV-1 showed that for the narrowband around its signature ($23 < f < 24$ Hz), the RMS acceleration level in this band was around 10 μg_{RMS} when it was off and around 40 μg_{RMS} when it was on.

8.3 Experiment Equipment

Support Equipment characterization related to different experiments performed on ISS during Increments 2 to 4 is the focus of this section.

8.3.1 GASMAP Sample Catheter Pump and Fan

In an effort to correlate accelerations measured in the US Lab to nearby operating equipment, correspondence with Human Research Facility (HRF) and Gas Analysis System for Metabolic Analysis of Physiology (GASMAP) teams was pursued to track down timeline information as well as equipment operational characteristics. The correspondence that ensued along with some data analysis resulted in the identification of two narrowband signatures near 60 Hz that were positively attributed to GASMAP equipment. This equipment was located in the HRF rack #1, in US Lab Starboard, Bay 2 (LAB1S2). The first, and stronger of the two, signatures identified was that of a sample catheter pump. The nominal operating range of this pump is 52-60 Hz. The second, somewhat weaker signature, belonged to the GASMAP fan, which typically operates at 58.3 Hz or 3500 rotation per minute (RPM). Timeline information from HRF activities such as rack (de)activation, ultrasound, and

PC data downlink did not yield discernible acceleration signatures in the SAMS measurements.
The spectrogram of Figure 18 shows the acceleration spectra for SAMS SE 121F02 in the Remote Triaxial Sensor (RTS) drawer 1 of LAB1O2. As discussed with GASMAP payload developers, the frequency changes away from nominal operation near 60 Hz are likely a function of varying loads on the sample pump. The pump frequency ranges from 54 Hz (for brief calibrations) up to 62 Hz after the second Pulmonary Function in Flight (PuFF) run. The fan is tightly controlled in frequency but also transitions from baseline of about 57.4 Hz up to 58.1 Hz during calibrations.

To assess the impact of the sample pump, 8-second interval RMS accelerations that span 8 hours around run time were computed and shown in Figure 19 for sensor 121F02. Comparing Figure 19 to similar figures for other SAMS data, it is noted that sensor 121F02 registers the largest impact of the 3 sensors analyzed. If we consider times when the pump frequency stayed in a relatively narrow band around nominal operation, we can tabulate more detail regarding the impact comparing times when the pump was off versus on as done in Table 10.

8.3.2 MEPS PCM Insertion and Runs

The Microencapsulation Electrostatic Processing System (MEPS) was located in locker #8 of ER1 (LAB1O2) in close proximity to the SAMS 121F02 sensor in RTS drawer 1. On GMT 18-July-2002 (day 199), the MEPS processed 5 samples and on GMT 19-July-2002 (day 200), another 3 samples were processed. According to the MEPS staff, the sample processing requires insertion of the Process Chamber Module (PCM). An interval maximum analysis shows transients including one that extends above 103 mg from a baseline of about 3 mg for PCM insertion. The SAMS 121F02 timestamps show this large pulse occurred at GMT 18-July-2002, 199/15:12:29. For a broader perspective, a 24-hour spectrogram that readily shows these impulsive disturbances from PCM insertion was computed and shown in Figure 20. This exhibit clearly delimits the 5 runs with the start/stop of 2 narrowband signals. The weaker of these was centered at 47.1 Hz and the stronger at 52.8 Hz. Note that each of the 5 runs is preceded by the impulsive events of PCM insertion.

The interval RMS versus time plot of Figure 21 corresponds to the same time frame as that of Figure 20. This RMS plot shows the contribution of the 2 narrowband signals that accompany the MEPS runs. The (red) trace gives the RMS acceleration for the fainter, low-frequency signal centered at 47.1 Hz. This signal steps from about 14 to 24 μg_{RMS} in the frequency range from 45.85 to 47.39 Hz. Likewise, the red trace for the stronger signal centered at 52.8 Hz steps from about 9 to 54 μg_{RMS} in the frequency range from 52.63 to 53.07 Hz.

8.3.3 Advanced AstroCulture

The Advanced AstroCulture (ADVASC) experiment has 2 fans, 2 blowers, and a pump among its payload equipment. Vibratory disturbances attributable to the payload fans can be qualified from the spectrograms of Figure 22 and Figure 23. ADVASC was located in ER1. The impact of ADVASC on the environment was measured by HiRAP. Table 11 shows the frequency range and measured acceleration levels for the different supporting machinery of the ADVASC experiment.

8.3.4 Experiment of Physics of Colloids in Space

Nominal sample mix operations in the Experiment of Physics of Colloids in Space (EXPPCS) test section produce a strong broadband disturbance near the mixer. Otherwise, farther away, a narrowband disturbance is dominant with fundamental of 12 Hz and harmonics, especially 9th harmonic at 108 Hz. The sample mixer typically operates with a 50%, 30-second duty cycle.

To quantify, the SAMS 121F06, which was mounted on EXPPCS test section (~1½ ft. from mixer in ER2) routinely measured peak accelerations in excess of 200 mg for a cutoff frequency of 100 Hz. For other SAMS sensors, like 121F03 and 121F04 mounted on the Z-panel of ER2 and ER1, the peak accelerations were 22 mg and 10 mg, respectively. Figures 24 and 25 show a spectrogram and an interval minmax illustrating the impact of EXPPCS on the environment as recorded by HiRAP and SAMS 121F06, respectively.

9 Increments 2 to 4 Grand Summary

The objective of the Increments 2 through 4 grand summary is to present to the microgravity scientific community a summary of the ISS microgravity environment magnitude levels during the period of May 2001 to April 2002. During that period over half a terabyte of acceleration data were collected and processed. This section presents and discusses the results of much of that half terabyte of data that were processed and analyzed. Results are presented for both the quasi-steady and the vibratory regimes.

Before any processing, the measured data was divided into their respective increment (Increments 2, 3 and 4) using each increment time demarcation (see Table 1). Each increment data set was further divided into different subsets to reflect different STS flights that occurred during that specific increment in order to account for the delivery of science facilities, new experiments, and the station buildup components within that increment. Five subsets of data were processed. Increment-2 was divided into two data subsets: data subset 1, which covered flight 6A and data subset 2, which covered flight 7A period (see Table 1 and Figure 3 for station components and experiment facilities delivered during these flights.) Increment-3 was divided into data subsets 3 and 4. These two data subsets covered flights 7A.1, 4R and UF-1. Increment-4 had one data set (data set 5), which covered flight 8A. For the vibratory analysis, all events were included in the analysis, such as EVAs, dockings, undockings. The only exception was the Space Shuttle/ISS joint operations. At assembly complete, during microgravity mode, these events should not take place. Therefore, the results presented in this grand summary for the vibratory response represents the worst-case scenario since both "microgravity mode" and non-microgravity modes are taken into account for this analysis. For the quasi-steady analysis results, the data was filtered to 0.01 Hz to take into account only relevant events to the quasi-steady regime.

Over half a terabyte of measured acceleration data aboard the ISS were archived and much of that processed for five SAMS SEs and MAMS-OSS from the period of May 2001 to April 2002. For the vibratory response, the data was divided into crew sleep and wake periods to assess the impact of crew motion and experiment operation versus crew sleep. In order to perform this analysis, many spectrograms were generated. Each spectrogram covers an 8-hour span. Therefore, three spectrograms were generated for each day for the entire period mentioned above for all five SAMS SEs (each combined 24-hour spectrogram contains approximately 300 MB of data for each sensor—depending on the sensor sample rate). Each spectrogram was visually inspected to select crew sleep and crew wake periods for each day. Once the time periods were selected, histograms were computed for each data subset within an Increment and combined to give a simple measure of "near worst case" conditions. The measure that was used is an approximate 95th percentile extracted from the cumulative percentage of occurrence for the combined histogram. Histograms for each data subset within an Increment were combined for that Increment overall 95th percentile. Finally, each histogram generated for each Increment was combined to generate the super-Increment (Increments 2 to 4) 95th percentile histogram.

The same process was used for the quasi-steady regime, except that the data was not separated into crew sleep and wake periods. Instead, the data was divided into LVLH and X-POP segments to assess the effect of these two station attitudes on the quasi-steady environment. Also, the X, Y and Z-axes were treated separately.

9.1 Quasi-steady Grand Summary

The ISS quasi-steady requirement (frequency less than 0.01 Hz) at assembly complete calls for an acceleration magnitude less than or equal to 1 micro-g and the component perpendicular to the orbital average acceleration vector to be less than or equal to 0.2 micro-g. Assembly complete configuration is still several years away. The purpose of the results presented in this section is to give Principal Investigators (PIs) a useful set of data, which can be used in their preliminary sensitivity analysis for their experiment. Tables 13-and 14 show the results of the quasi-steady grand summary for the acceleration data collected by MAMS-OSS over approximately one year. The tables show the mean along with its deviation for the 95th percentile for both LVLH and XPOP attitudes at the MAMS-OSS location, in the ISS analysis coordinate system. Table 13 shows the attitudes effect for each data subset within each Increment. Table 14 shows similar results, each Increment as well as for all of the 4 Increments combined (Increments 2 to 4). The results consistently show that the LVLH attitude yields a lower quasi-steady environment for the X-axis compared to the XPOP attitude. However, the Y and Z-axes are consistently better when ISS is in XPOP attitude than LVLH. The reason the X-axis is better for the LVLH attitude than XPOP is due to the gravity gradient and rotational components canceling out along that axis. In XPOP, the X-axis is perpendicular to the orbital plane and is predominantly the gravity gradient effect since ISS is not rotating with respect to the inertial coordinate system. The reason the Y and Z-axes are lower in magnitude in XPOP than LVLH is because the overall quasi-steady vector direction changes (cyclic), making the average come out close to zero (the Y and Z-axes are subjected to varying drag and gravity gradient components as the ISS completes an orbit). In LVLH, however, the overall quasi-steady vector is pointing in the same direction for both the Y and Z-axes throughout the orbit. Also, another factor that needs to be taken into account when comparing quasi-steady components for different attitudes of a

spacecraft is the distance of the sensor from the orbiting vehicle center of mass (CM). MAMS-OSS is located much closer to the CM of the ISS in the Y and Z-axes than in the X-axis. Distance to the CM is less of an impact for the X-axis component in LVLH attitude since gravity gradient and rotational effects cancel out. The data collected during the Increments 2 to 4 period clearly shows that. Table 15 shows some ancillary data such as number of hours of acceleration data processed and number of samples points for each data subset (and configuration) for each increment and the overall total hours of acceleration data analyzed for Increments 2 to 4.

9.2 Vibratory Grand Summary

The ISS vibratory requirement at assembly complete calls for:

1. for $0.01 \leq f \leq 0.1$Hz: $a \leq 1.6$ µg
2. for $0.1 < f \leq 100$ Hz: $a \leq f \times 16$ µg
3. for $100 < f \leq 300$ Hz: $a \leq 1600$ µg

Where "f" is frequency and "a" is acceleration. Even though the results presented in this section are not for assembly complete and do not meet the measurement location and the microgravity mode condition specified in the microgravity control plan document, the results are, nevertheless, useful to PIs for experiment sensitivity assessment as well as to the vehicle PIs interested in the transfer functions or transmissibility assessment. Every effort was made to give the PIs all the necessary information (racks locations and dimensions in the US LAB, US LAB dimensions, sensor locations and relative distance from each other, sensors distance from the racks geometric centers) to facilitate such assessment and calculations.

Tables 16 through 18 show the results of the vibratory grand summary for the acceleration data collected by the five SAMS SEs over approximately one year. Table 16 shows the results for each data subset within each increment for crew sleep, crew wake and the combined crew sleep and wake (both) conditions. Table 17 shows similar results, but for each increment as well as for the combined case of all three increments. Also, Table 17 contains some ancillary information such as cutoff frequency for each sensor that was analyzed, facility to which each sensor was attached to, and the number of hours of data that were analyzed for each sensor. Table 18 shows the actual plots from which Table 17 was generated. It gives the reader a much more comprehensive view of the acceleration magnitude on the ISS. The reader can easily see where, for example, 50% or 80% of the time the acceleration magnitude level was for a specific sensor for sleep, wake and both conditions combined for each increment as well as for all three increments combined. On the top part of each plot, the Increment #, the condition (for example, sleep), and the 95th percentile value are listed. On the left corner of the plot, the sensor name and its cutoff frequency are listed. On the right corner, total number of hours of acceleration data processed for the plot is listed. A few things need to be pointed out regarding the values reported in Tables 16 and 17. First, when only wake or sleep data exists, the same value is reported under the column "both". Second, The acceleration values in the tables are in milli-g (10^{-3}) and they are approximately (sometimes higher, but never lower) the 95th percentiles extracted from each histogram for each case. The reason the value listed is not always exactly 95th percentile is due to the acceleration magnitude bin resolution (the next higher bin value was consistently used as the reported values). The alternative was to linearly interpolate the actual value. Third, the sensors cutoff frequencies are not all the same. This point is very important for the sleep and wake comparison. Finally, the reader is urged to refer to Figures 2 and 3 as well as Tables 2 and 3 for proper context and understanding of the results presented in Tables 16 through 18.

It is clear from the results that the acceleration levels (magnitude) measured by sensor 121F02 during the period of this study are consistently higher than all of the other sensors. The second in rank is 121F04 followed by 121F03 and 121F06 is the quietest. 121F02 has the highest measured magnitude levels because its cutoff frequency is 2 times higher than both 121F03 and 121F04. The noisiest equipment or dominant frequencies were in the 100 plus Hertz. Both 121F03 and 121F04 cutoff frequencies are 100 Hz and both are attached to the ISS structure and are 42 inches apart, however, 121F04 is consistently louder than 121F03. This is due to the equipment (fans, pumps, blowers) operating in ER-1 in support of a specific experiment and also to the transmissibility path characteristic between ER-1 and 2. Both F05 and F06 were expected to report much lower acceleration levels since their cutoff frequency is much lower than the other three sensors. In the case of F05 and F06 only the activities under 25 Hz, such as crew activities, crew exercise and life support equipment that operate within that frequency spectrum, contributed to the levels reported. Another important point is the acceleration level values listed for sleep and wake. The magnitude levels reported for sleep are sometimes higher than the wake's periods. There are two reasons for that. The case labeled "sleep" is NOT truly sleep in a strict sense of the word. To truly consider sleep, the data under

consideration would have to be either recorded at 5 Hz and below or filtered at 5 Hz and below since this is the frequency spectrum relevant to sleep period. The data recorded and presented in Tables 16 through 18 was not recorded or filtered as mentioned above. Therefore, all the equipment operating in the higher frequencies (above 5 Hz to 200 Hz) dominate. Consequently, the real impact of the sleep period (is lost) is masked by the higher frequencies. For example, for Increment-3, the 121F02 sensor, whose cutoff frequency is 200 Hz, has a 95th percentile magnitude level of 3.75 mg for sleep compared to wake's 3.65 mg. Since the life support equipment, experiment hardware, science facilities equipment are operating during the sleep period and dominate above 20 Hz, the quiescent environment provided by the sleep period at 5 Hz and below is nullified by the dominance of the equipment operating above 20 Hz. The second reason sleep is higher than wake is because for that specific case, there were more hours recorded (at higher magnitude levels) for that sensor (and processed) for sleep than wake period. A good illustration of the points made above regarding the higher frequency dominance that nullified the quiescent environment provided by crew sleep period are the results from 121F05 and 121F06 sensors. Since they were set at 25 Hz (still too high of a cutoff to capture the true sleep period benefit, but much better compared to 121F02), the acceleration magnitude level for the sleep period is much lower (more than one order of magnitude lower). Also, one would expect the acceleration magnitude levels during the sleep period to be consistently lower than wake's, which is, indeed, the case for sensor 121F05.

To really show the impact of sleep vs. wake, one subset of data from sensor 121F03 was filtered to 5 Hz and below. Table 19 shows the comparison between 121F03 sensor set at a cutoff frequency of 100 Hz for sleep, wake and both conditions and the case for which F03 sensor data was filtered to 5 Hz and below, thereby eliminating the influence of all the higher frequencies. The real benefit of the sleep period can now be assessed. As before, for the 100 Hz case, 95th percentile for sleep is 2.23 mg, 2.15 mg for wake and 2.20 mg for both combined. For the 5Hz case, the 95th percentile for sleep is 0.06 mg, 0.20 mg for wake and 0.17 for both combined.

The implication to PIs is the following. If an experiment is sensitive to 5 Hz and below, then that experiment will benefit from operating during crew sleep and /or during Public Affair Office (PAO) events. The PAO period has the same effect of crew sleep since the crew is not active. Even if an experiment is sensitive to 25 Hz and below, operating such experiment during crew sleep is still beneficial. However, if an experiment is sensitive to 100 Hz and below, it does not make much difference whether such experiment is run during crew sleep or not since the higher frequencies dominate.

A word of caution about the results for F06 sensor is in order here. F06 was mounted in ER-2, which is an actively isolated rack. During the period the data was collected for F06, the isolation system was being validated on orbit. Therefore, different tests were conducted for such validation. The rack was not always in isolation mode and due to the different tests and rack configurations, a lot of high transient magnitude levels were seen in the collected data. Due to lack of available information regarding the actual status (modes) the rack was in during the period of this study and lack of human resources to match specific modes with specific time hacks from such a huge amount of data, no definite technical judgment can be made for 121F06, except to say that the acceleration magnitude levels presented in Tables 16 through 18 represent the worst case in term of "active" isolation performance for 121F06. It must be pointed out that the sensor 121F06 was mounted on the ER2, therefore it was actively isolated at times, whereas 121F05 was mounted on the upper Z-panel of ER2, above the rack, therefore it was not actively isolated. The acceleration magnitude levels recorded by these two sensors are fairly comparable.

10 Acknowledgments

The authors would like to acknowledge a number of people whose work contributed significantly to this paper. Without their work, this paper would have not been possible. Significant contributions were made in the area of software development, the Microgravity Analysis Software System (MASS), which enabled both MAMS and SAMS to acquire acceleration data aboard the ISS, process, analyze, and display the data on the PIMS website as well as systems troubleshooting, by Nissim Lugasy, Ted Wright, and Eugene Liberman. We would like to acknowledge also the development efforts of the SAMS-II team and the MAMS project team/Canopus, Inc. The authors would like to thank Timothy Reckart for his contribution to this work. Finally, we would like to thank John Keller (JSC) and Ted Bartkowicz (Boeing, ISS Loads and Dynamics) for TVIS exercise and other timeline information that proved invaluable for correlation with acceleration measurements; Janelle Fine (University of California at San Diego Department of Medicine Physiology/NASA Laboratory) for PuFF operations notes from her console logbook; Jake Fox, Joel Falcon,

and Clifton Amberboy (Lockheed Martin) for GASMAP equipment operations, information and characteristics; The ISS Payload Rack Officer (PRO) on console personnel, the ISS Attitude Determination and Control Officer (ADCO) on console personnel who provided the authors with valuable timeline information

11 References

1. International Space Station: Expedition 5— Building Scientific Momentum, USA/Boeing/NASA, May 16, 2002.

2. Hamacher, H., "Low-Frequency Residual Acceleration", Journal of Spacecraft and Rockets, Vol. 32, No. 2, pp. 324-327, 1995.

3. DeLombard, Richard., "Microgravity Requirements Scientific Research on the International Space Station", soon to be published as a NASA-Technical Memorandum

4. International Space Station, "Microgravity Control Plan", SSP 50036, Rev. B, February 15, 1999

5. DeLombard, Richard., "Compendium of Information Pertaining to the International Space Station Microgravity Acceleration Environment", NASA-TM (to be assigned soon)

6. Space Acceleration Measurement System II, RTS SE Electronic Test Report, SE 121-Q02, SAMS-II 657-RPT1, NASA, December 2000

7. "Microgravity Acceleration Measurement System for the International Space Station", Canopus System Inc., CSI 0101 MAMS TR-008, Contract No: NAS3-26556, May 2001

8. International Space Station User's Guide Release 2.0, NASA

9. International Space Station Coordinate Systems, SSP-30219, Revision F

10. K. Jules et al, "International Space Station Increment-2 Microgravity Environment Summary Report", NASA/TM-2002-211335, January 2002

11. K. Jules et al, "International Space Station Increment-3 Microgravity Environment Summary Report", NASA/TM-2002-211693, June 2002

12. K. Jules et al, "International Space Station Increment4/5 Microgravity Environment Summary Report", NASA/TM-, (to be assigned soon)

13. 5th Annual Microgravity Environment Interpretation Tutorial (MEIT), NASA-PIMS, Volume 1, Section 7, March 5-7, 2002

14. Alan V. Oppenheim, Ronald W. Schafer, Digital Signal Processing, Prentice-Hall, Inc., New Jersey, 1995

15. Julius S. Bendat, Allan G. Piersol, Random Data: Analysis and Measurement Procedures, Wiley-Interscience, New York, 1986

16. Melissa J. B. Rogers, Kenneth Hrovat, Summary Report of Mission Acceleration Measurements for STS-87, NASA/TM-1999-208647

17. ICD-A-21438-OOR, Space Flight Operations Contract, Mission ISS 7A.1 Orbiter/ISS On-Orbit Cargo Element Interfaces, ICD-A-21438-OOR, Prepared by The Boeing Company, Human Space Flight and Exploration Under Subcontract 1970483303, PDRD P1226, May 7, 2001, DRD-1.2.2.6 Contract NAS9-20000

ACRONYM	DEFINITION
ADVASC	*Advanced AstroCulture*
ATL	*Attitude Timeline*
CDT	*Central Daylight Time*
CEVIS	*Cycle Ergometer with Vibration Isolation System*
CM	*Center of Mass*
CST	*Central Standard Time*
DC	*Direct Current (steady)*
DC-1	*Russian Docking Compartment*
ER	*EXPRESS rack*
EVA	*Extra-Vehicular Activity*
EXPPCS	*EXPeriment of Physics of Colloids in Space*
EXPRESS	*EXPedite the PRocess of Experiments of the Space Station*
GASMAP	*Gas Analysis System for Metabolic Analysis of Physiology*
Geom	*Geometric*
GRC	*Glenn Research Center*
HiRAP	*High Resolution Accelerometer Package*
HRF	*Human Rack Facility*
Hz	*Hertz*
ISIS	*International Subrack Interface Standard*

ISS	*International Space Station*	*PCM*	*Process Chamber Module*
IVA	*Intra-Vehicular Activity*	*PCSA*	*Principal Component Spectral Analysis*
JSC	*Johnson Space Center*		
LAB	*Laboratory*	*PI*	*Principal Investigator*
LAB	*U.S. Laboratory Module*	*PIMS*	*Principal Investigator Microgravity Services*
MAMS	*Microgravity Acceleration Measurement System*	*PSD*	*Power Spectral Density*
MASS	*Microgravity Acceleration Software System*	*PuFF*	*Pulmonary Function in Flight*
		R	*Russia*
MBS	*Mobile Base System*	*ROS*	*Russia Orbital Segment*
MEP	*Microgravity Environment Program*	*S0*	*S-zero Truss*
		SAMS	*Space Acceleration Measurement System*
MEPS	*Microencapsulation Electrostatic Processing System*	*SE*	*Sensor Enclosure*
		SM	*Service Module*
NASA	*National Aeronautics and Space Administration*	*STS*	*Space Transportation System*
		TEA	*Torque Equilibrium Attitude*
OARE	*Orbital Acceleration Research Experiment*	*TMF*	*Trimmed Mean Filter*
		TVIS	*Treadmill with Vibration Isolation System*
OBPR	*Office of Biological and Physical Research*	*U.S.*	*United States of America*
OSS	*OARE Sensor Subsystem*	*USOS*	*United States Orbital Segment*
ossbtmf	*OSS TMF*	*XPOP*	*X Principal Axis Perpendicular to the Orbit Plane*
ossraw	*OSS raw data*		
PAD	*PIMS Acceleration Data*		

Table 1 Missions to ISS and Increments Configuration Changes For Increments 2 through 4

	INCREMENT-2	INCREMENT-3	INCREMENT-4
Shuttle	STS-102 / STS-100 / STS-104 / STS-105	STS-105 / Soyuz / STS-108	STS-108/STS-110/STS-111
Mission	5A.1 / 6A* / 7A§ / 7A.1	7A.1 / 4R* / UF-1	UF-1 / 8A* / UF-2§
Docking date	March 10, 2001/April 21, 2001/July 13, 2001/August 12, 2001	August 12, 2001/September 17, 2001/December 7, 2001	December 7, 2001/April 10, 2002/June 7, 2002
Docking time (CDT)	12:38 AM± /8:59 AM / 10:08 PM / 01:42 PM	01:42 PM / 6:05 AM / 02:03 PM	02:03PM/11:05AM/11:25AM
Undocking date	March 18, 2001/April 29, 2001/July 24, 2001/August 20, 2001	August 20, 2001/September 26, 2001/December 15, 2001	December 15, 2001/April 17, 2002/June 15, 2002
Undocking time (CDT)	10:32 PM± / 12:34 AM/ 11:54 PM/ 09:52 AM	09:52 AM /10:36 AM./ 11:28 AM	11:28PM/01:31PM/09:32AM
Special cargo	*Delivery and installation of the Canadarm2 to ISS § Delivery and installation of Quest Airlock to ISS	* Delivery of the Docking compartment-1 (DC-1), Pirs, and the Strela Boom	* Delivery and installation of the S0 (S-zero) Truss to ISS § Delivery and installation of the Mobile Base System (MBS) to ISS

± Central Standard Time (CST)

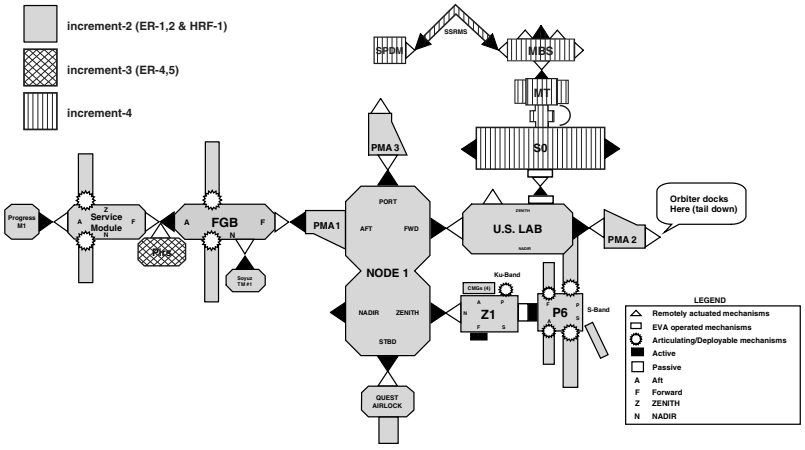

Figure 1. ISS Increments 2 Through 4 Layout

Table 2. Sensors Locations (in inch) Relative to ER Geometric Center and ISS-USOS/US LAB Coordinates

	ISS-USOS-Analysis Coordinate (SSA)			US LAB Coordinate System			Δ from Forward Hatch (in SSA)			Δ from ER1 Geom Center (in SSA)			Δ from ER2 Geom Center (in SSA)		
	X	Y	Z	X	Y	Z	X	Y	Z	X	Y	Z	X	Y	Z
121F02	128.73	-23.53	144.15	808.44	23.54	-46.80	119.84	23.54	-46.80	14.97	23.54	10.20	56.97	23.54	10.20
121F03	191.54	-40.54	135.25	745.63	40.56	-55.70	57.03	40.56	-55.70	-47.84	40.55	1.30	-5.84	40.55	1.30
121F04	149.54	-40.54	135.25	787.63	40.56	-55.70	99.03	40.56	-55.70	-5.84	40.55	1.30	36.16	40.55	1.30
121F05	185.17	38.55	149.93	752.00	-38.54	-41.02	63.40	-38.54	-41.02	-41.47	-38.54	15.98	0.53	-38.54	15.98
121F06	179.90	-6.44	145.55	757.27	6.45	-45.40	68.67	6.45	-45.40	-36.20	6.45	11.60	5.80	6.45	11.60
OSS	135.28	-10.68	132.12	801.89	10.69	-58.83	113.29	10.69	-58.83	8.42	10.69	-1.83	50.42	10.69	-1.83
HiRAP	138.68	-16.18	142.35	798.49	16.19	-48.60	109.89	16.19	-48.60	5.02	16.19	8.40	47.02	16.19	8.40
F. H (1)	248.57	0.01	190.95	688.60	0.00	0.00	0.00	0.00	0.00	-104.9	0.00	57.00	-62.87	0.00	57.00
ER2 (2)	164.95	-40.36	150.57	772.22	40.37	-40.38	83.62	40.37	-40.38	-21.25	40.37	16.62	20.75	40.37	16.62
ER2 (3)	185.70	0.01	133.95	751.47	0.00	-57.00	62.87	0.00	-57.00	-42.00	0.00	0.00	0.00	0.00	0.00
ER1 (4)	122.95	-40.36	150.57	814.22	40.37	-40.38	125.62	40.37	-40.38	20.75	40.37	16.62	62.75	40.37	16.62
ER1 (5)	143.70	0.01	133.95	793.47	0.00	-57.00	104.87	0.00	-57.00	0.00	0.00	0.00	42.00	0.00	0.00

Note (1): Forward Hatch; **Note (2**): EXPRESS Rack-2 front lower left corner; **Note (3)**: EXPRESS Rack-2 geometric center; **Note (4):** EXPRESS Rack-1 front lower left corner; **Note (5):** EXPRESS Rack-1 geometric center

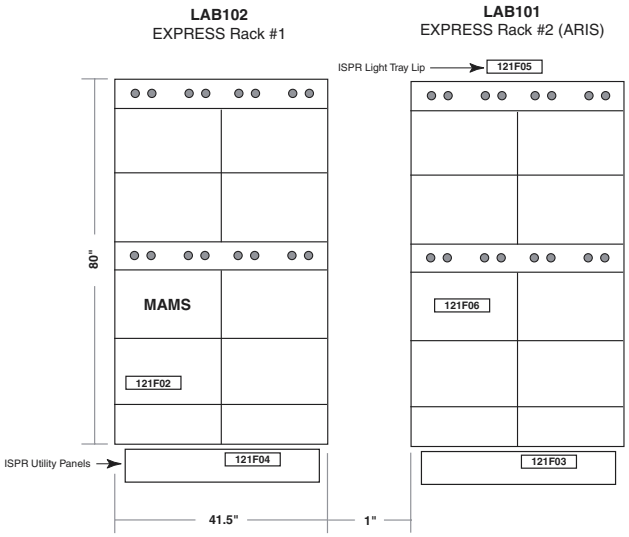

Figure 2. MAMS and SAMS Accelerometers Locations on/in ER 1 and 2 During Increments 2 to 4

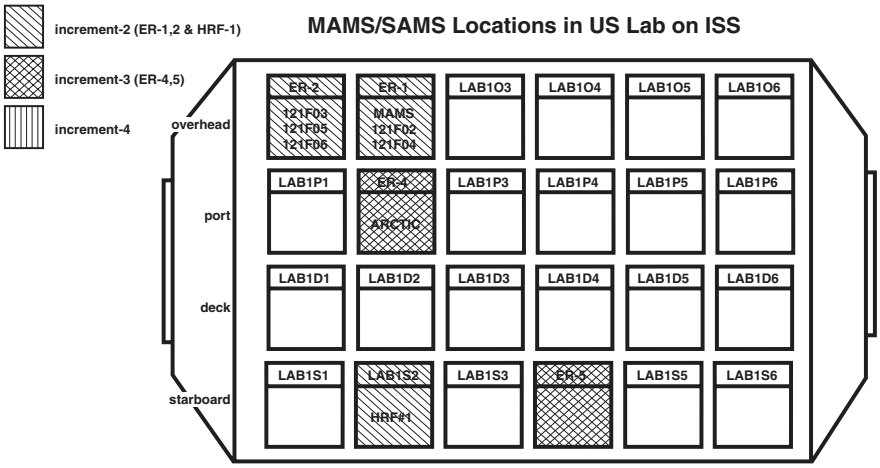

Figure 3. ER 1 and 2 Locations in the US LAB for Increments 2 to 4 Configurations

Table 3. Sensors Overall Distance (Magnitude—in inch) in the U.S LAB Coordinates

	121F02	121F03	121F04	121F05	121F06	OSS	HiRAP
121F02		65.677	28.312	84.105	53.964	18.78	12.5
121F03	65.677		42.00	80.699	37.478	63.772	58.636
121F04	28.312	42.00		87.987	46.806	33.243	27.604
121F05	84.105	80.699	87.987		45.514	72.322	72.213
121F06	53.964	37.478	46.806	45.514		46.788	42.474
OSS	18.78	63.772	33.243	72.322	46.788		12.102
HiRAP	12.50	58.636	27.604	72.213	42.474	12.102	

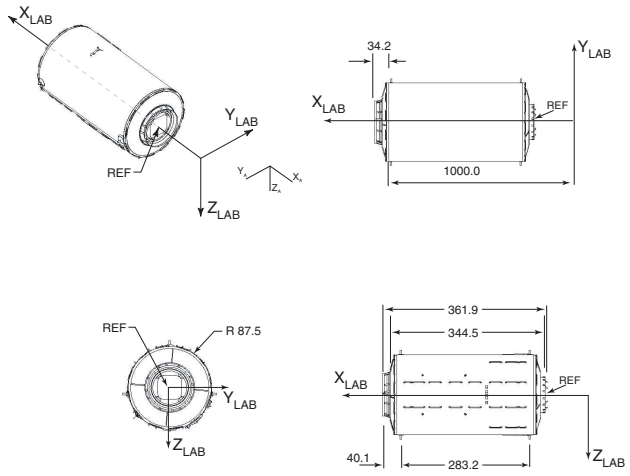

Figure 4. U.S LAB "Destiny" Dimension and Coordinate System

Table 4. Acceleration Data Archived Per Sensor From May 2001- May 2002

Month	Gigabytes of Acceleration Data Archived*										
	SAMS					SAMS	MAMS			MAMS.	NASA GRC
	121F02	121F03	121F04	121F05	121F06		HiRAP	ossbtmf	ossraw		
May-01	0.000	0.000	0.000	0.000	0.000	0.000	3.594	0.001	0.327	3.921	3.921
Jun-01	1.087	3.801	1.381	1.350	3.449	11.068	8.355	0.001	0.236	8.592	19.659
Jul-01	2.363	7.898	7.133	3.997	11.245	32.636	15.870	0.002	0.522	16.394	49.030
Aug-01	5.133	11.161	6.871	3.179	7.920	34.263	33.444	0.002	0.591	34.037	68.301
Sep-01	2.250	9.982	5.144	2.212	5.983	25.571	28.016	0.002	0.422	28.440	54.011
Oct-01	16.052	13.657	13.771	4.713	17.985	66.177	27.548	0.002	0.607	28.157	94.335
Nov-01	17.443	10.453	10.589	1.738	6.282	46.503	6.921	0.002	0.562	7.486	53.989
Dec-01	11.676	5.220	5.209	1.450	0.847	24.401	2.544	0.002	0.451	2.996	27.398
Jan-02	17.067	8.910	8.635	2.545	2.750	39.907	1.394	0.002	0.577	1.974	41.881
Feb-02	16.480	8.280	7.380	1.967	2.288	36.396	0.524	0.002	0.504	1.030	37.425
Mar-02	12.350	6.221	6.146	8.442	7.123	40.284	3.592	0.002	0.554	4.148	44.432
Apr-02	6.194	3.049	2.750	1.689	0.571	14.254	7.362	0.002	0.442	7.806	22.059
May-02	10.568	11.744	8.797	3.437	0.827	35.373	7.364	0.002	0.580	7.946	43.319
Total	118.66	100.38	83.806	36.719	67.270	406.83	146.53	0.026	6.375	152.927	559.76

* From May 2001 to May 2002 (approximately one year) PIMS has archived over half a terabyte of acceleration data from ISS (Increments 2 to 4), approaching about 50,000 hours (for all the sensors combined).

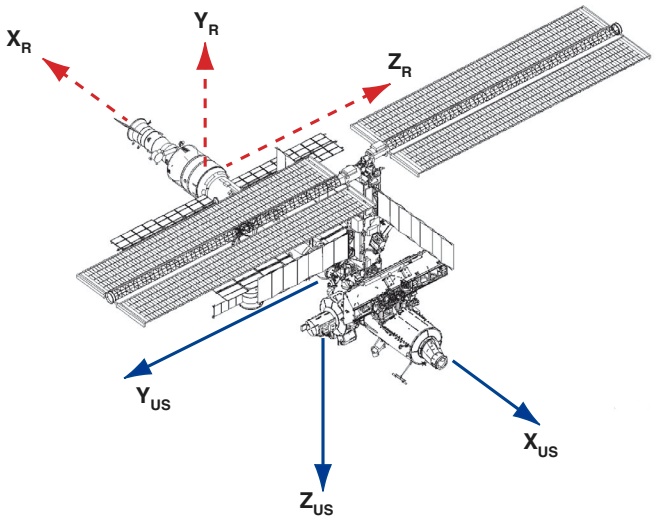

Figure 5. ISS-USOS / ROS Analysis Coordinate Systems

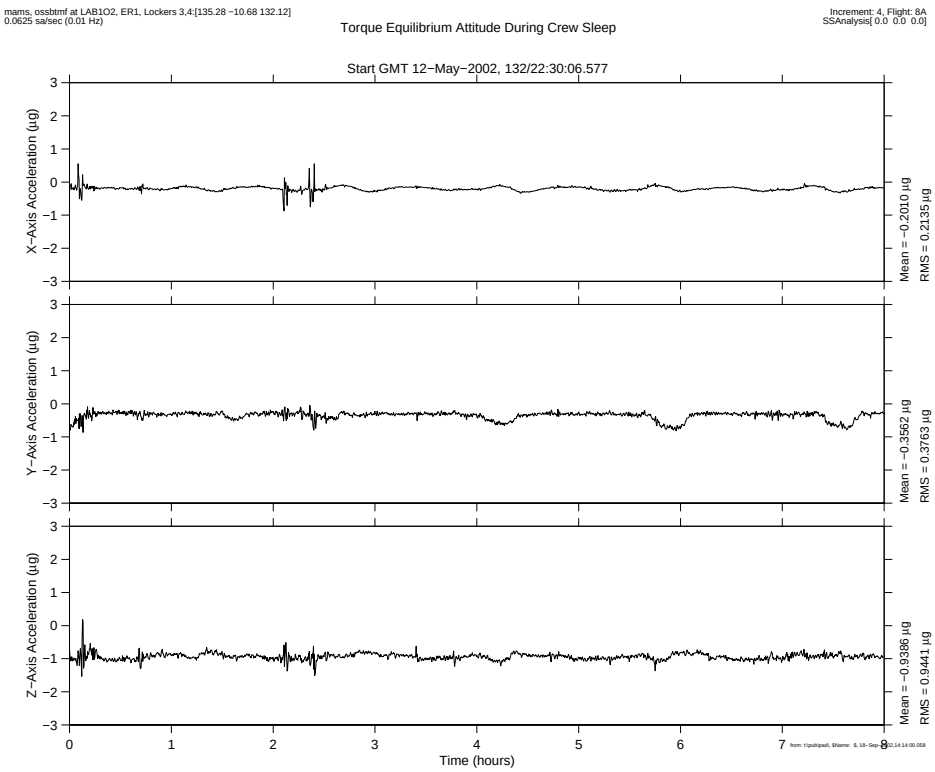

Figure 6. Torque Equilibrium Attitude (TEA)

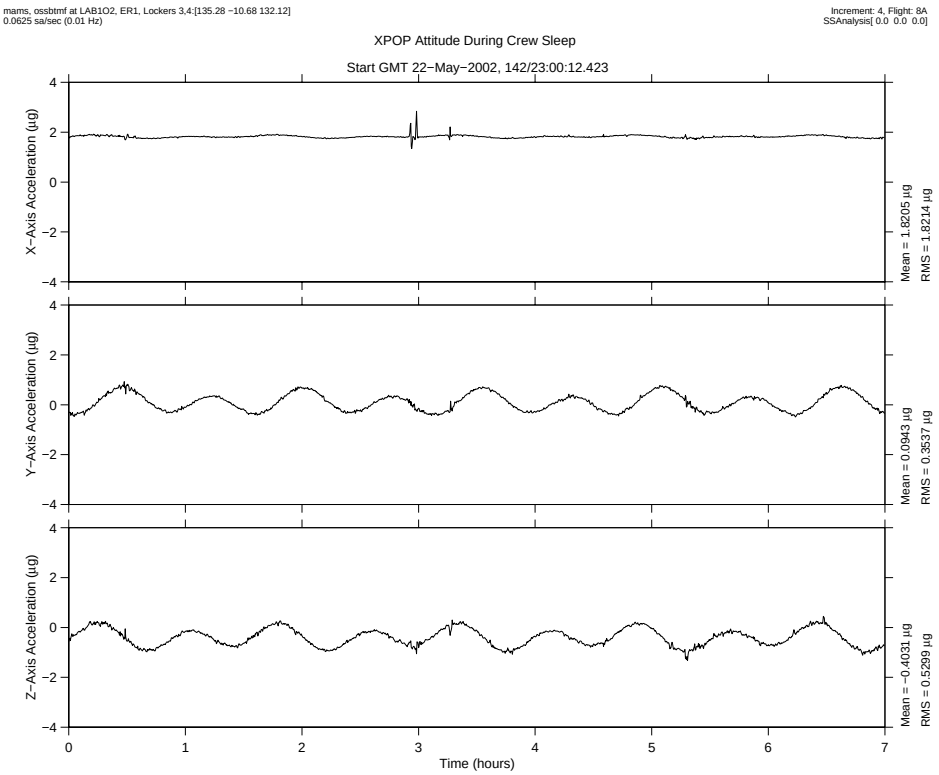

Figure 7. X Principal Axis Perpendicular to the Orbit Plane (XPOP)

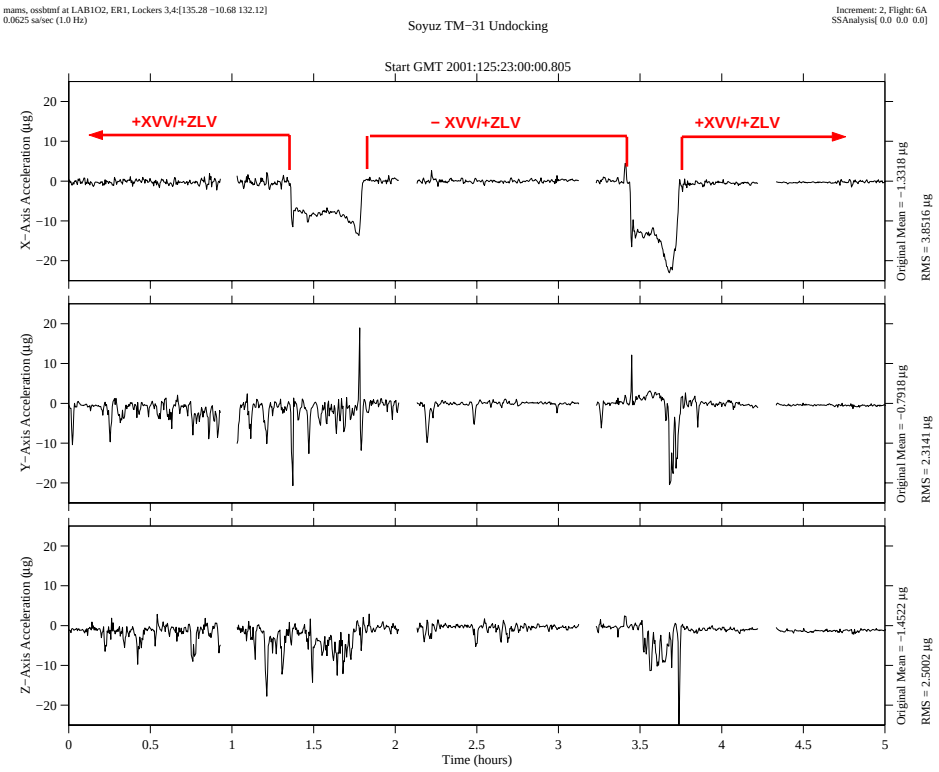

Figure 8. TM-31 Undocking

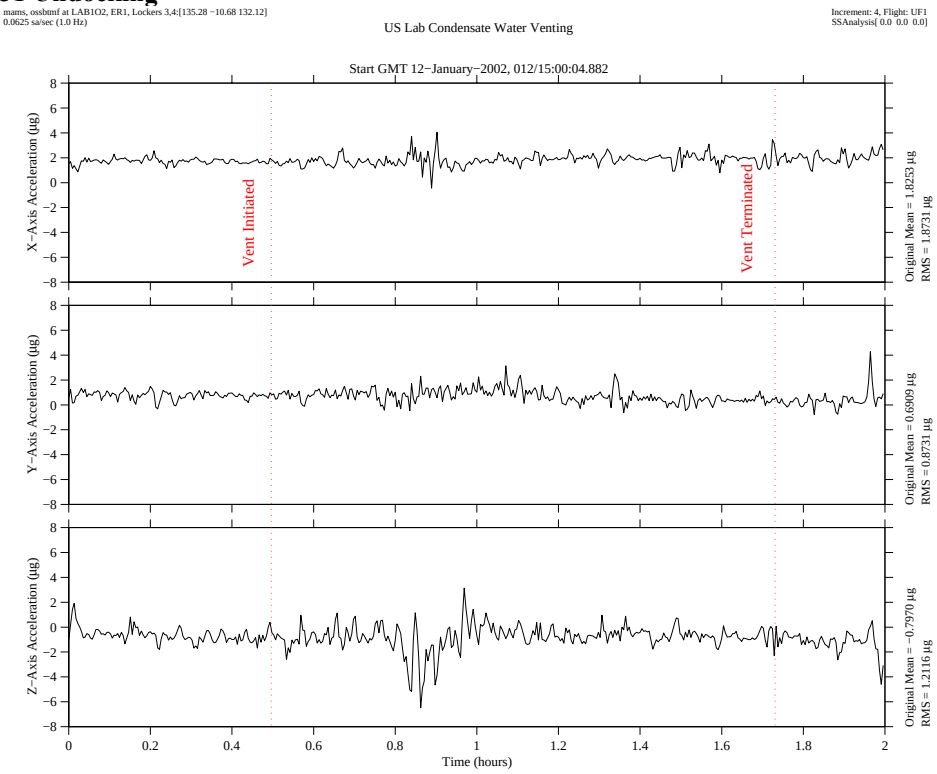

Figure 9. U.S LAB "Destiny" Water Venting

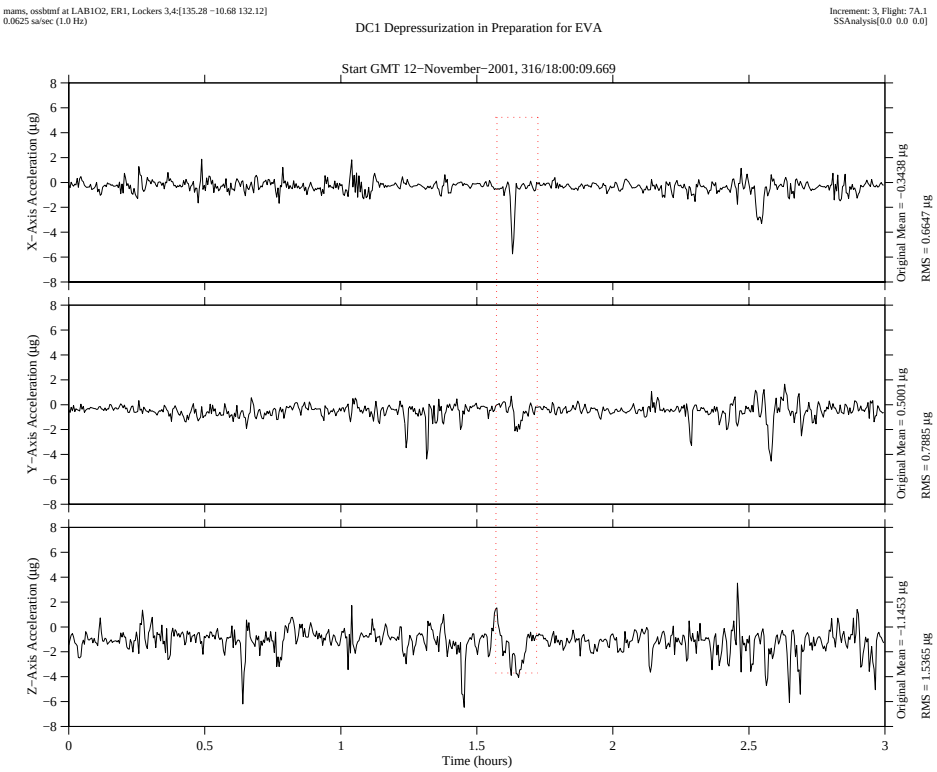

Figure 10. DC-1 (Pirs) Depressurization

Table 5. Quasi-steady Events Measured During Increments 2 to 4

Source	Effect	GMT
Soyuz TM-31 Undocking	12 μg peak in X_A direction	06-May-2001, 126/00:19:58
Progress (4P) Docking	10 μg peak in X_A , Y_A direction	23-May-2001, 143/00:24:23
STS-104 (7A) Docking	6 μg peak magnitude	14-July-2001 03:21:04
STS-105 (7A.1) Docking	5 μg peak magnitude	12-Aug-2001 224/19:02:35
STS-105 (7A.1) Undocking	6 μg peak magnitude	20-Aug-2001 232/14:52:00
STS-105 Joint Ops	2.9 μg Mean magnitude	12-Aug-2001 224/19:00:00
Progress 4P Undocking	10-20 μg peak in - X_A direction	22-August-2001, 234/06:07:00
DC1 Docking	10-25 μg in - X_A direction	17-September-2001, 260/01:05:00
CMG 2 Testing	Increased variation on X_A, Y_A, and Z_A axes.	11-October-2001, 283/04:50:00
Soyuz 2 Relocation	8-10 μg peak in - X_A direction	19-October-2001, 291/07:58:00
EVA Activities	12-18 μg peak in -Y_A, and -Z_A directions.	08-October-2001, 281/14:23 12-November-2001, 316/21:41
SSRMBS Maneuvers	7-13 μg in the -X_A, and -Z_A directions.	08-October-2001, 281/14:23
DC1/PkhO Depressurization	4 μg peak in -X_A direction 1.5 μg peak in -Y_A direction	08-October-2001, 281/14:23 12-November-2001, 316/02:35
Thrusters Inhibited Recovery	10-20 μg in –X_A direction for extended period	03-December-2001, 337/13:20
Progress 5P Prop Purge	3.5 –5.7 μg in Y_A, and -Z_A directions.	20-November-2001, GMT 234/19:10
USLab Water Dump	6 μg peak in Z_A direction.	12-January-2002, GMT 012/15:30

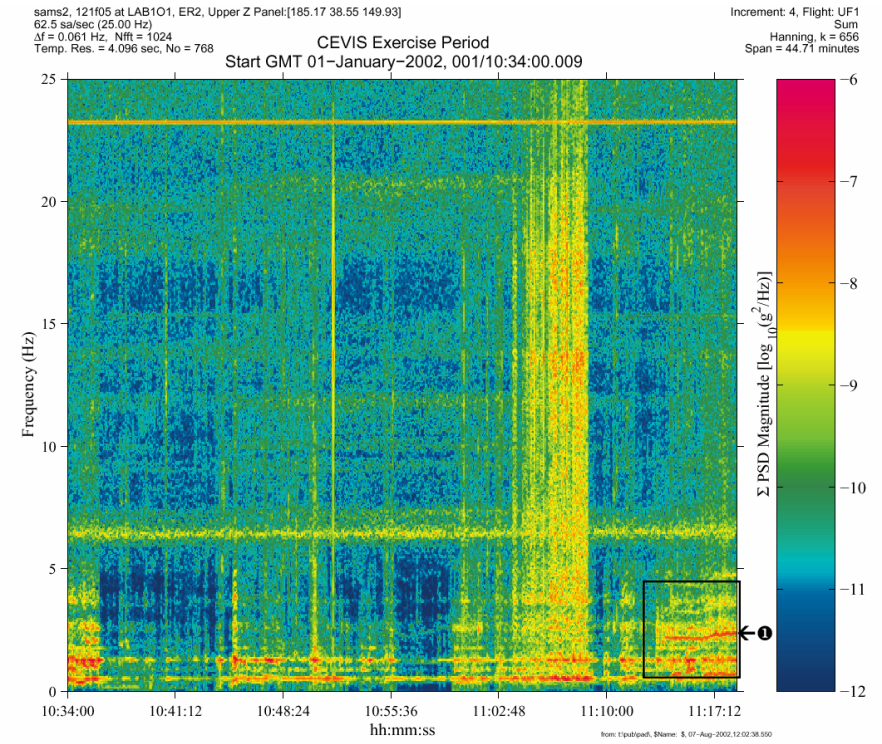

Figure 11 Spectrogram of CEVIS Exercise Period (121F05)

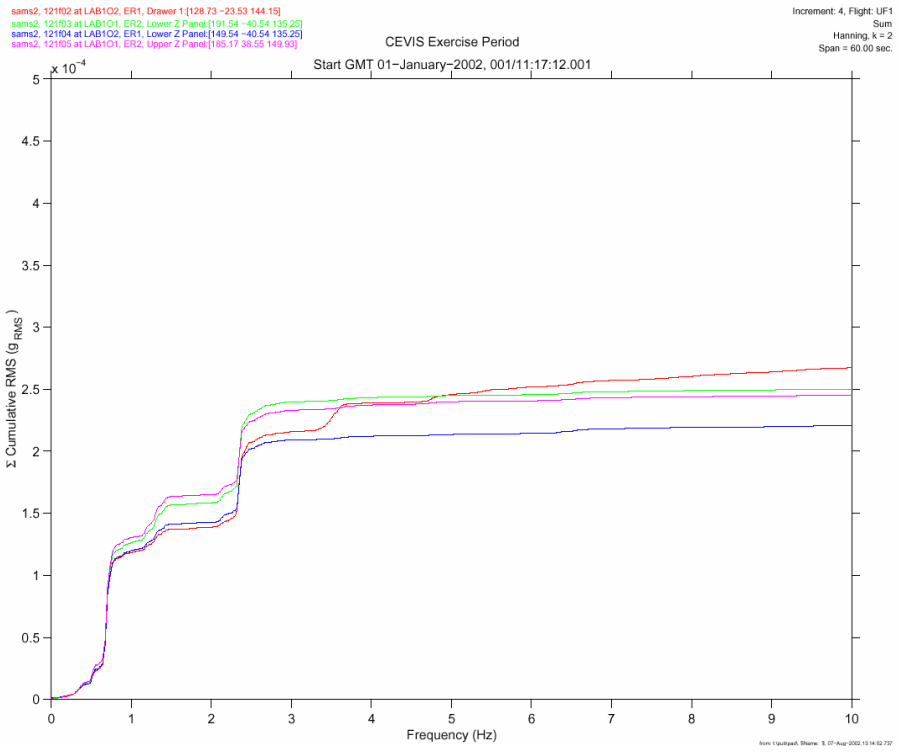

Figure 12 Cumulative RMS of CEVIS Exercise Period (121F02, 121F03, 121F04, 121F05)

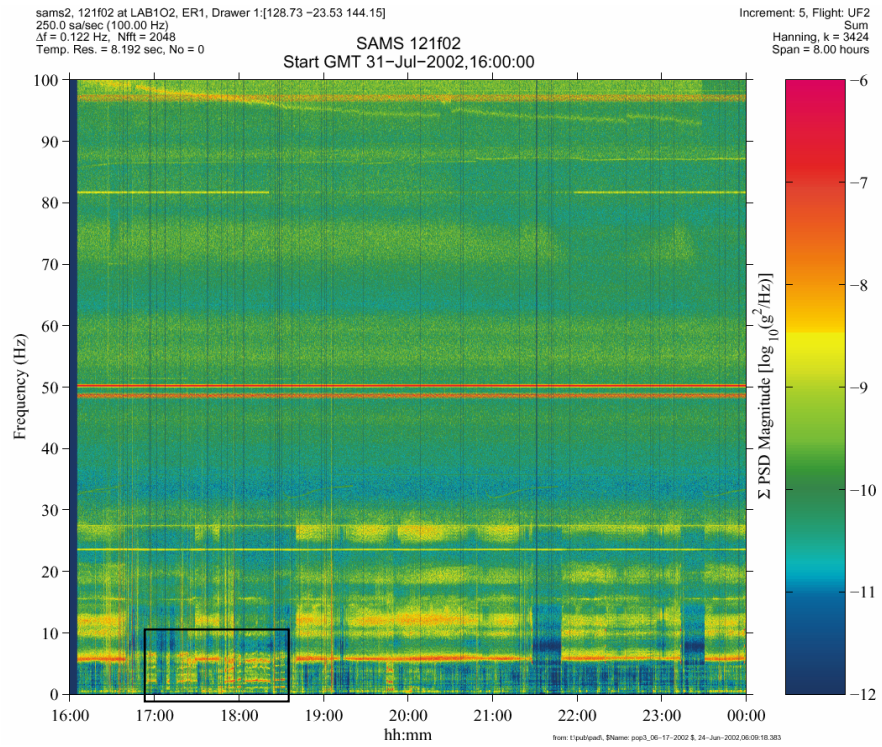

Figure 13 Spectrogram of Velo Exercise Periods (121F02)

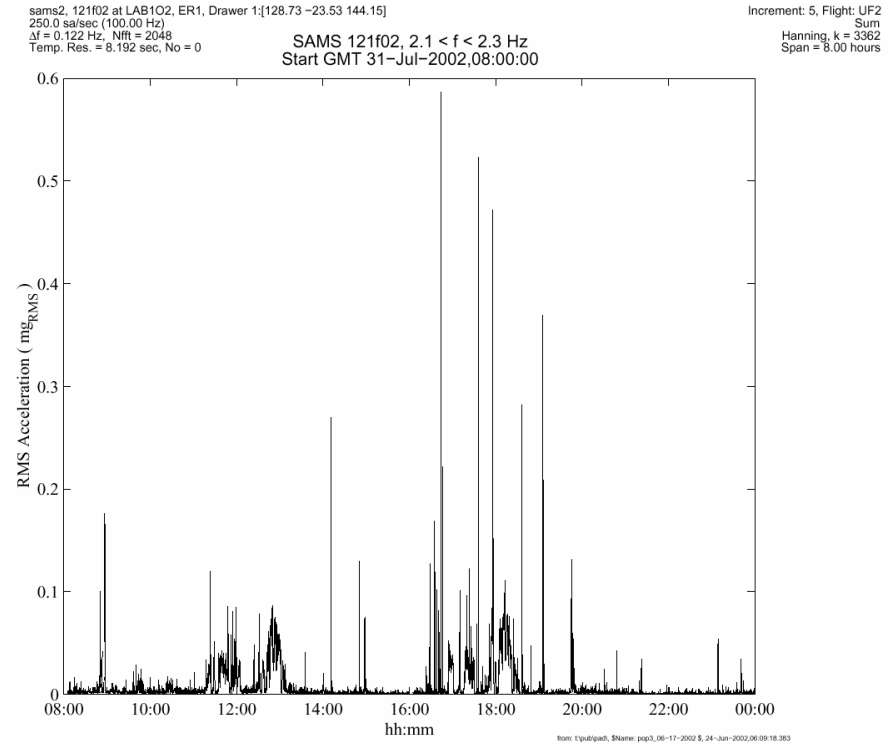

Figure 14 Interval RMS of Velo Exercise Periods (121F02)

Table 6 Excerpt of "Inc 4A As-Flown ISS Attitude Timeline (ATL)

#	MANEUVER START-STOP (GMT)	BETA ANGLE	ATTITUDE NAME	REF FRAME	YAW PITCH ROLL	EVENT	REMARKS
194	065/01:34 01:36	-38	+ZLV +XVV	LVLH	359.5 357.9 0.0	Mnvr to UF1 Stage Reboost 3 Attitude	Burn Start 03:37:12.00 Burn Stop 03:39:50.20
195	065/03:42 03:43	-37	+ZLV +XVV	LVLH	359.5 357.9 0.0	Mnvr to UF1 Stage Reboost 4 Attitude	Burn Start 04:29:07.00 Burn Stop 04:35:42.10
201	071/22:04 22:06	-5	+ZLV +XVV	LVLH	359.5 357.9 0.0	Mnvr to UF1 Stage Reboost 5 Attitude	Burn start: 00:04:10.00 Burn stop: 00:09:29.00
202	072/00:12 00:13	-4	+ZLV +XVV	LVLH	359.5 357.9 0.0	Mnvr to UF1 Stage Reboost 6 Attitude	Burn start: 00:52:49.00 Burn stop: 01:03:25.10

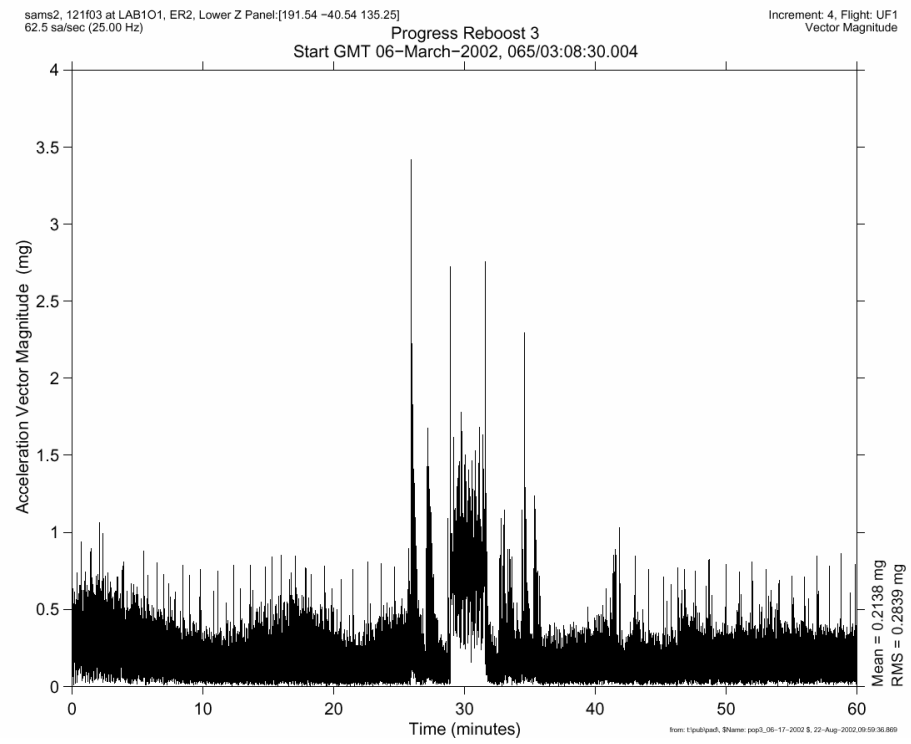

Figure 15 Acceleration Magnitude of Progress Reboost 3 (121F03)

Table 7 Progress Reboost Median Acceleration Magnitude Comparison

Sensor	Cutoff Frequency (Hz)	Location	State	Median Acceleration Vector Magnitude (µg)
121F02	25	LAB1O2, ER1, Drawer 1	Not During Burn 3	284
			During Burn 3	745
121F03	25	LAB1O1, ER2, Lower Z Panel	Not During Burn 3	155
			During Burn 3	769
121F04	25	LAB1O2, ER1, Lower Z Panel	Not During Burn 3	181
			During Burn 3	747
121F02	25	LAB1O2, ER1, Drawer 1	Not During Burn 4	313
			During Burn 4	770
121F03	25	LAB1O1, ER2, Lower Z Panel	Not During Burn 4	159
			During Burn 4	758
121F04	25	LAB1O2, ER1, Lower Z Panel	Not During Burn 4	179
			During Burn 4	737

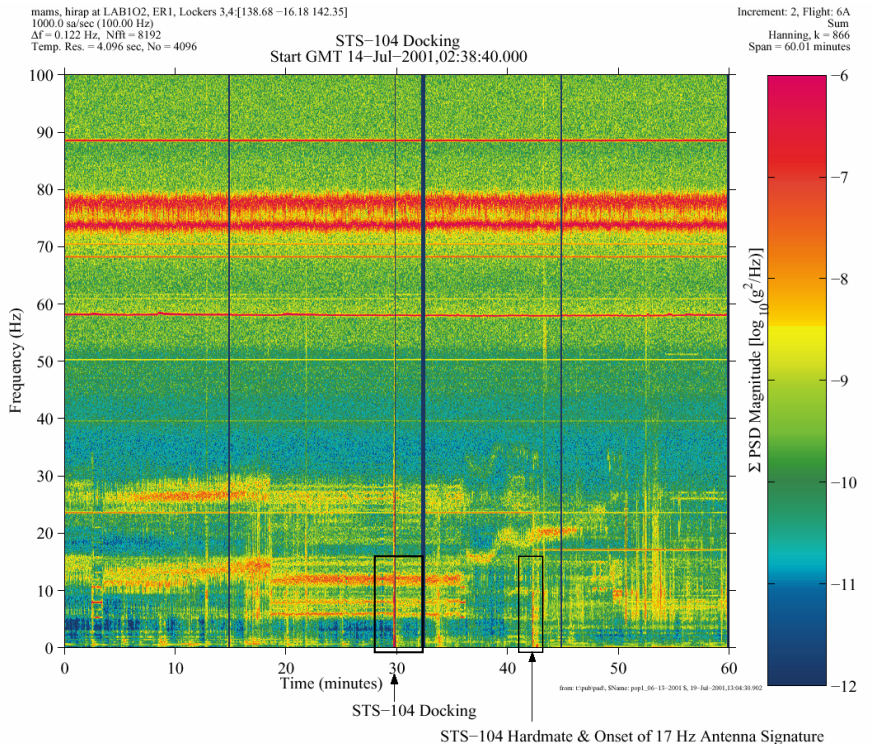

Figure 16 Shuttle (7A) Docking HiRAP Spectrogram

Table 8 STS-104, Flight 7A Ku-Band Antenna Dither Transmission

Event	GMT	Sensor	RMS Acceleration (16.93 < f < 17.13 Hz)
Before Hardmate	14-July-2001 03:17:34 - 03:19:34	MAMS HiRAP	0.6 μg_{RMS}

After Hardmate	14-July-2001 03:22:34 - 03:24:34		22.9 μg_{RMS}

Table 9 STS-104, Flight 7A Undocking Acceleration Magnitudes

GMT	Peak Magnitude (mg)
22-Jul-2001 04:54:26	7.5
22-Jul-2001 04:54:45	5.5
22-Jul-2001 04:54:55	5.4
22-Jul-2001 04:55:05	5.7
22-Jul-2001 04:55:15	5.0

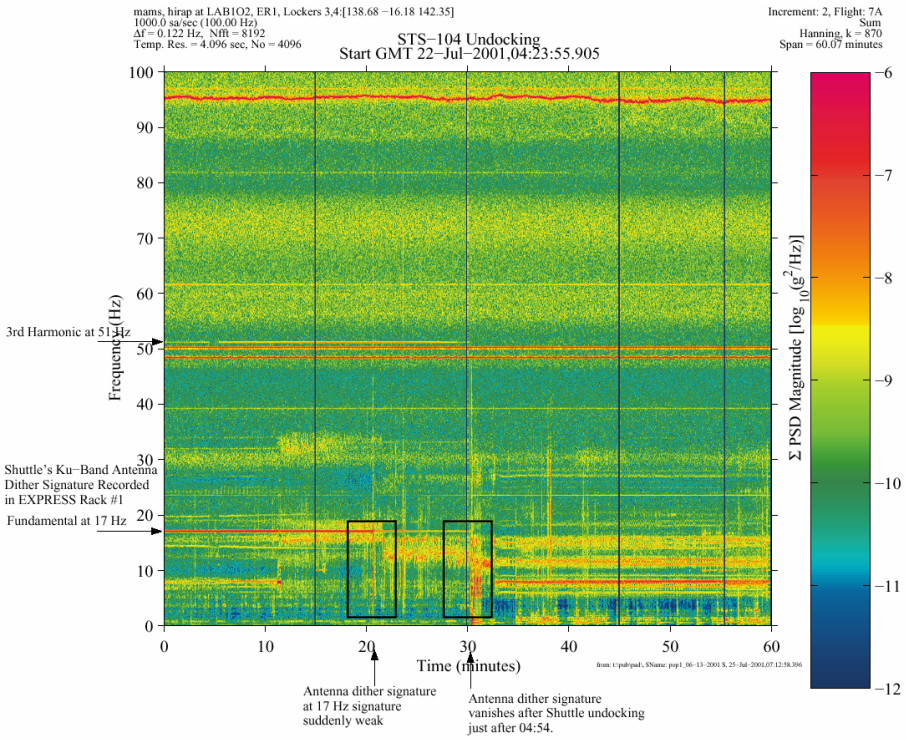

Figure 17 Shuttle (7A) Undocking HiRAP Spectrogram

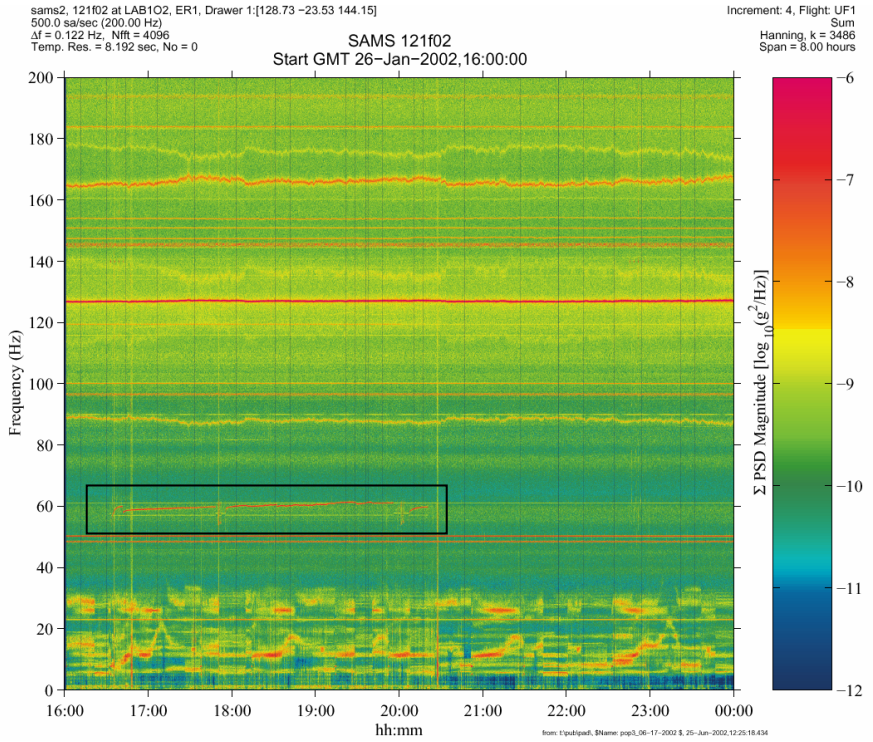

Figure 18 Spectrogram of GASMAP Equipment Operations (121F02)

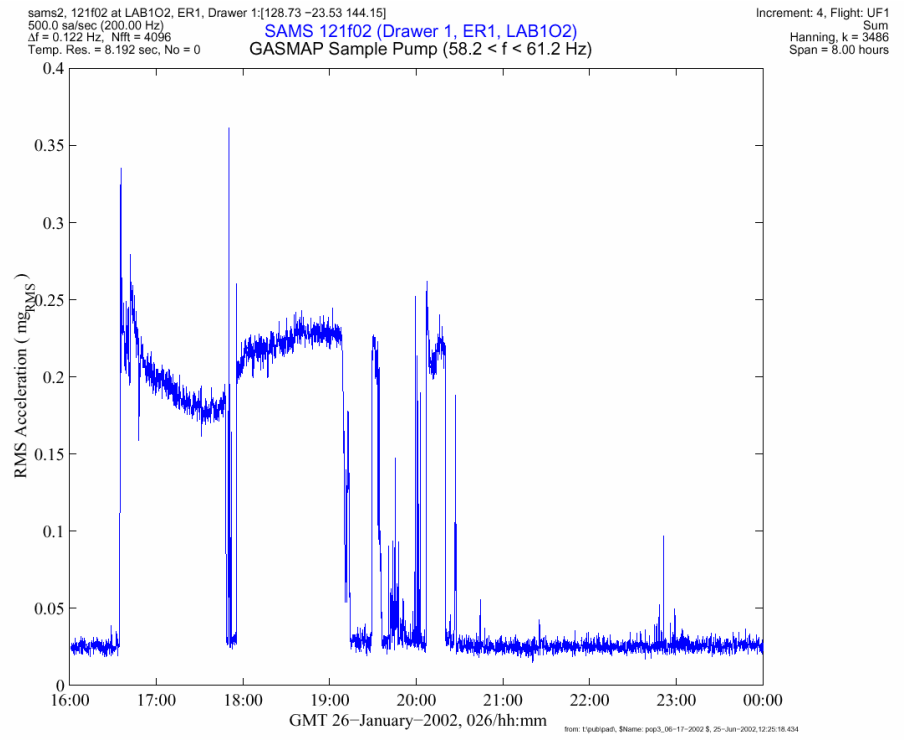

Figure 19 Interval RMS of GASMAP Sample Pump (121F02)

Table 10 GASMAP Equipment RMS Accelerations

Sensor	Location	Equipment	Frequency Range (Hz)	State	RMS Acceleration (μg_{RMS})
121F02	LAB1O2, ER1, Drawer 1	SAMPLE PUMP	58.2 – 61.2	OFF	24
				ON	>200
121F03	LAB1O1, ER2, Lower Z Panel			OFF	91
				ON	>115
121F04	LAB1O2, ER1, Lower Z Panel			OFF	70
				ON	>115
121F02	LAB1O2, ER1, Drawer 1	FAN	57.2 – 57.6	OFF	8
				ON	19

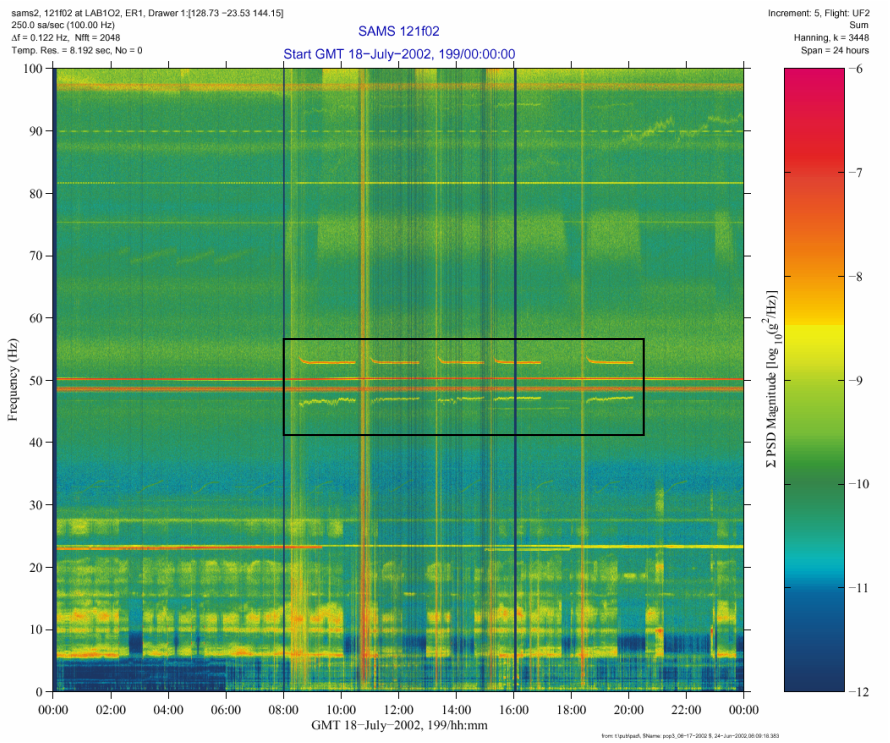

Figure 20 Spectrogram of 5 MEPS Runs (121F02)

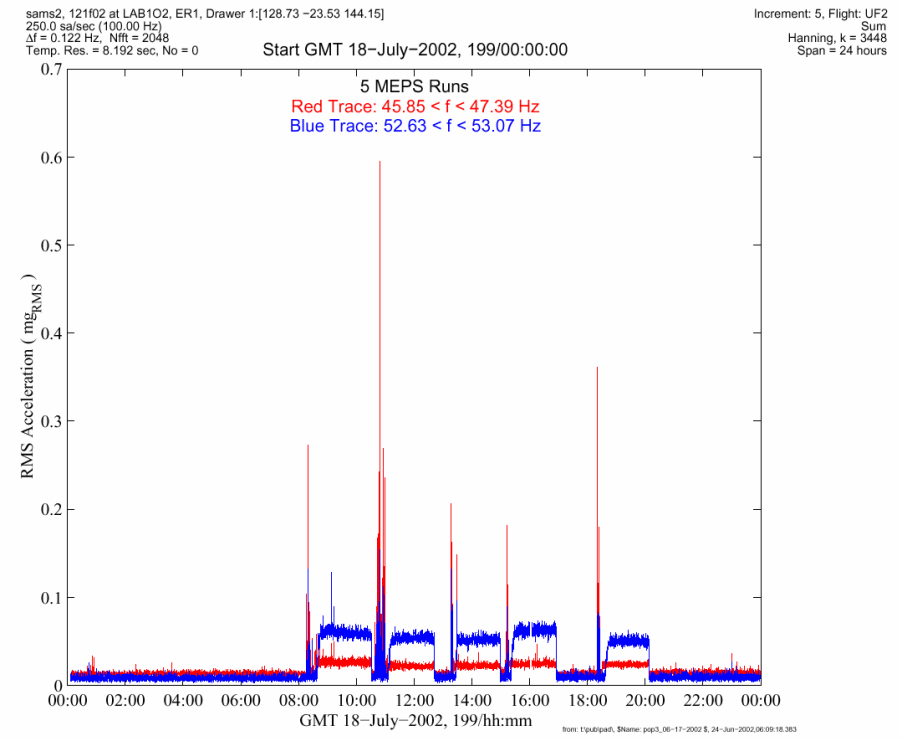

Figure 21 Interval RMS of 5 MEPS Runs (121F02)

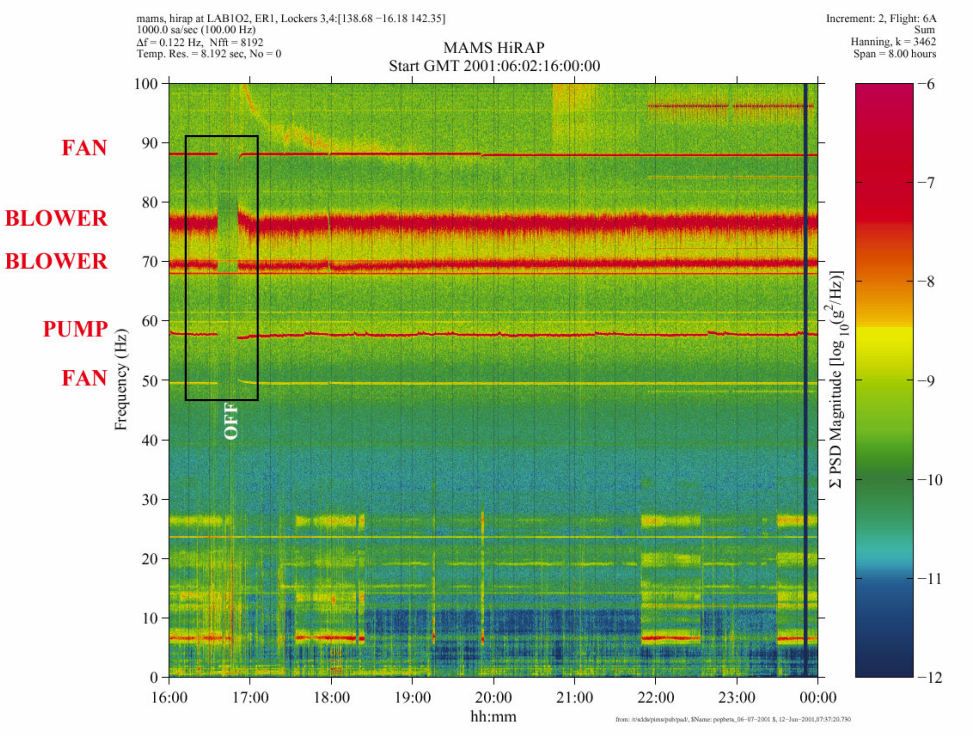

Figure 22 Spectrogram of ADVASC (HiRAP)

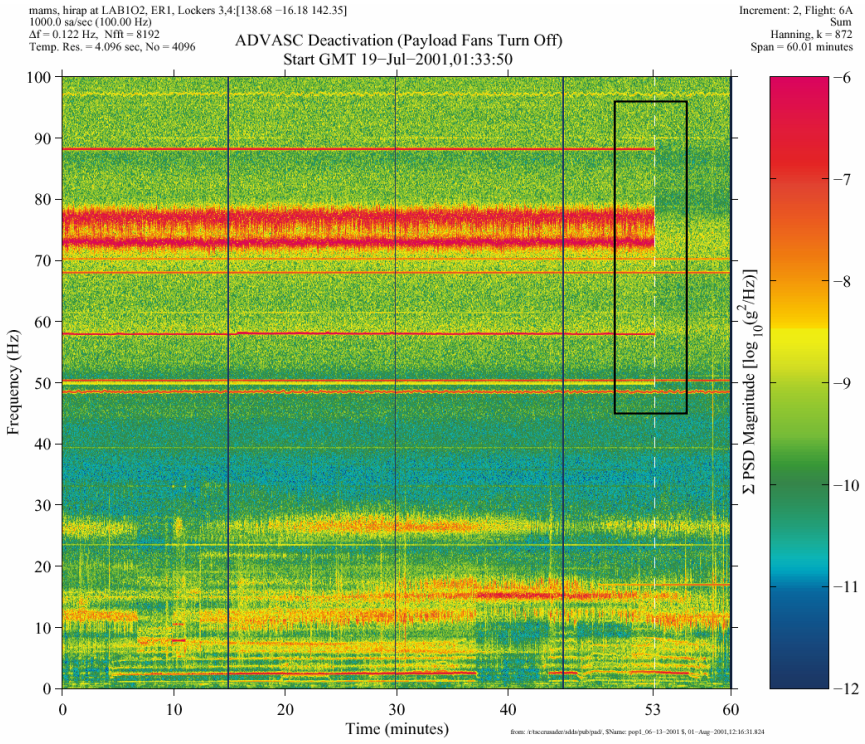

Figure 23 Spectrogram of ADVASC Deactivation (HiRAP)

Table 11 Snapshot of ADVASC RMS Acceleration Contributions

Frequency (Hz)			ADVASC Disturbance	RMS Acceleration (μg_{RMS})		Note
HiRAP Measured		Expected		ADVASC ON	ADVASC OFF	
Center	Range					
49.4	49.1 - 49.7	48.3	2900 RPM fan	41.6	19.0	narrowband
57.6	57.3 - 57.9	52 - 55	air pump	568.9	31.4	narrowband
67.9	67.6 - 68.1		no	120.7	115.7	narrowband
69.5	68.1 - 70.9	71.7	4300 RPM blower	512.9	97.4	broadband
70.1	69.7 - 70.3		no	202.3	71.4	narrowband
76.5	73.0 - 79.7	78.3	4700 RPM blower	940.9	86.9	broadband
88.0	87.6 - 88.4	88.3	5300 RPM CPU fan	284.3	32.8	narrowband

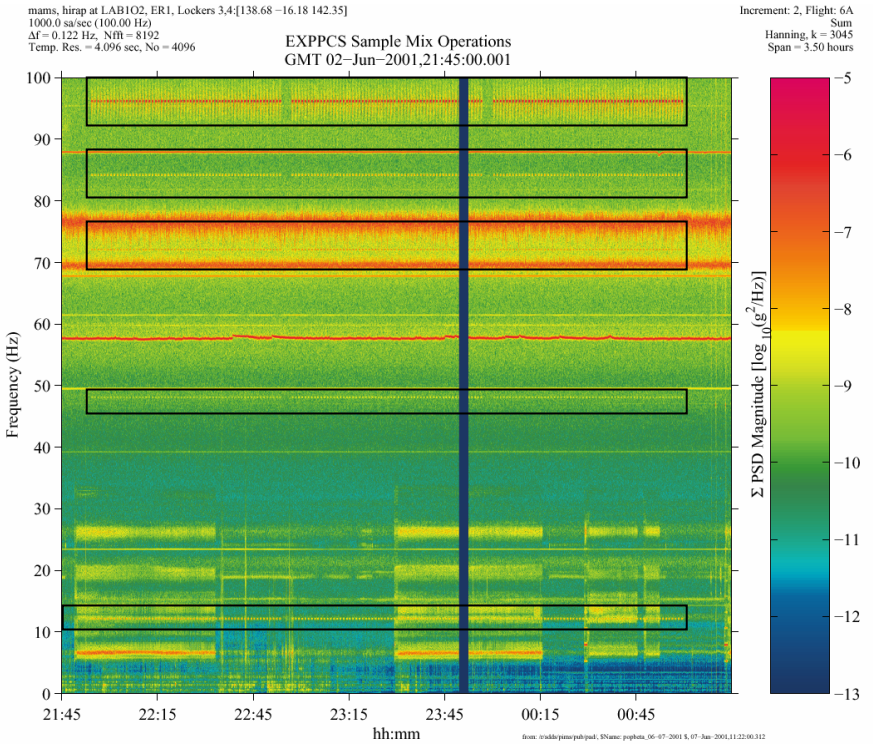

Figure 24 Spectrogram of EXPPCS Equipment Operation (HiRAP)

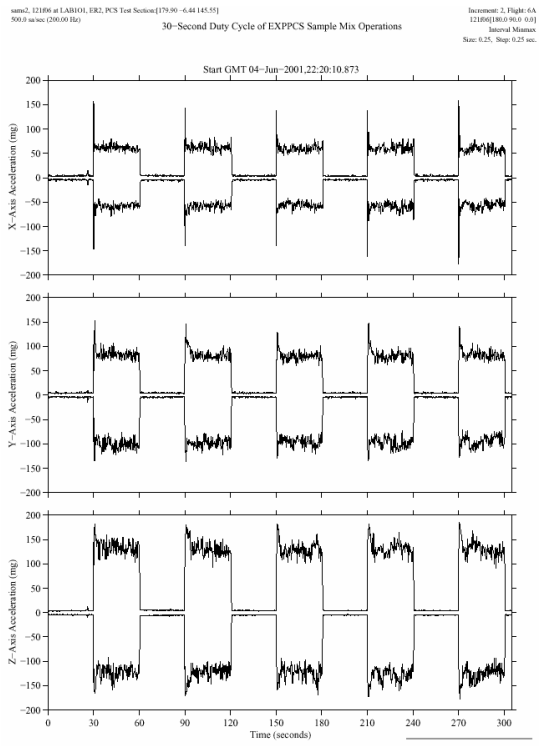

Figure 25 Interval Minmax of EXPPCS Operation

Table 12 ISS Increments 2 to 4 Events Characterization

Sensor	Source	Component	Frequency (Hz)	Range (Hz)	RMS (μg)	Peak (mg)	Bandwidth	State
CREW ACTIVITY								
121F02	Exercise	CEVIS		0-10	86		Narrowband	
121F05	Exercise	Velo		0-10	387		Narrowband	
121F05	Normal ops	TeSS entry/exit		0-200		15	Broadband	
121F05	Special ops	EVA-7		0-200		62	Broadband	
HiRAP	Normal ops			0.06-6	40		Broadband	Wake
HiRAP	Normal ops			0.06-6	9		Broadband	Sleep
121F02	Exercise	RED		0-10	301 (60)*			Squats
					691 (60)			Toe lifts
					336 (60)			Deep toe lifs
					206 (60)			Bar squats
					225 (60)			Bench press/pullups
					255 (60)			One-leg squats
VEHICLE								
121F02	ECLSS	SKV-1	23.5	23-24	8		Narrowband	Off
					37			On
HiRAP	Progress (4P)			< 100		13	Broadband	Dock
121F02	Progress (4P)			0-25		1.0	Broadband	Undock
HiRAP	Progress (5P)			0-25		2.0	Broadband	Thruster test
121F05	Progress (5P)			0-25		3	Broadband	Thruster test
121F06	Progress (5P)			0-25		3	Broadband	Thruster test
HiRAP	Progress (4P)			0-25		19	Broadband	Dock
121F03	Progress	Thrusters		0-25		1.0	Broadband	Reboost
HiRAP	Shuttle (7A)			< 100		10	Broadband	Dock softmate
						6		Dock hardmate
HiRAP	Shuttle (7A.1)			< 100		29	Broadband	Dock softmate
						14		Dock hardmate
EXPERIMENTS								
HiRAP	ADVASC	Fan (2900)	49.4	49.1-49.7	19		Narrowband	Off
					42			On
HiRAP	ADVASC	Air pump	57.6	57.3-57.9	31		Narrowband	Off
					569			On
HiRAP	ADVASC	Blower (4300)	69.5	68.1-70.9	97		Narrowband	Off
					513			On
HiRAP	ADVASC	Blower (4700)	76.5	73-79.7	87		Broadband	Off
					941			On
HiRAP	ADVASC	CPU fan (5300)	88.0	87.6-88.4	33		Narrowband	Off
					284			On
HiRAP	ADVASC	2 fans, 2 blowers, 1 pump		< 100	300			Off
					1000			On
121F06	EXPPCS	Sample mixer	12.0	< 100		237		On
121F03	EXPPCS	Sample mixer	12.0	< 100		22		On

Table 12 (Continue..) ISS Increments 2 to 4 Events Characterization

Sensor	Source	Component	Frequency (Hz)	Range (Hz)	RMS(µg)	Peak (mg)	Bandwidth	State
EXPERIMENT								
121F04	EXPPCS	Sample mixer	12.0	< 100		10		On
121F02	MAMS	Fan	183	182.3-183.7	32		Narrowband	Off
					96			On
HiRAP	SAMS	ISIS drawer # 1 fan	48.3	47.8-48.9	71		Narrow warble	On
Hirap	SAMS	ISIS drawer # 2 fan	50.2	50-50.4	88		Narrowband	On
121f02	GASMAP	Catheter pump	59.7	58.2-61.2	24		Narrowband	Off
					200			On
121F02	GASMAP	Fan	57.4	57.2-57.6	8		Narrowband	Off
					19			On
121F02	MEPS	Sample run: fan # 1 (?)	46.6	45.9-47.4	14		Narrowband	Off
					24			On
121F02	MEPS	Sample run: fan # 2 (?)	52.9	52.6-53.1	9		Narrowband	Off
					54			On
121F02	MEPS	PCM		0-100		103	Broadband	Insertion

*** Baseline acceleration level (before RED exercise session)**

Table 13. MAMS-OSS Trimmed Mean Filter Data Set Summary*

		Increment-2				Increment-3				Increment-4	
		Data subset 1		Data subset 2		Data subset 3		Data subset 4		Data set 5	
Attitude	Axis	Mean(µg)	± 95th	Mean(µg)	± 95th	Mean(µg)	± 95th	Mean(µg)	± 95th	Mean(µg)	± 95th (µg)
LVLH	x	-0.21	0.85	-	-	-0.16	0.85	-0.26	0.80	-0.32	0.75
	y	-0.89	1.00	-	-	-0.56	0.85	-0.58	1.00	-0.48	0.75
	z	-1.01	1.30	-	-	-0.91	1.50	-1.02	1.60	-0.96	1.25
XPOP	x	2.00	0.85	1.97	0.20	1.86	0.75	1.89	0.75	1.88	0.75
	y	-0.44	1.15	-0.06	0.60	0.07	1.15	-0.03	1.15	0.08	1.15
	z	-0.31	1.30	-0.49	0.65	0.58	1.75	-0.50	1.75	-0.25	1.45

* Acceleration values are in micro-g and data is being reported in the ISS-USOS Analysis Coordinates

Table 14. MAMS-OSS Trimmed Mean Filter Increments Summary*

		Increment-2		Increment-3		Increment-4		Increments-2/4	
Attitude	Axis	Mean(µg)	± 95th (µg)	Mean(µg)	± 95th (µg)	Mean(µg)	± 95th (µg)	Mean(µg)	± 95th (µg)
LVLH	x	-0.21	0.85	-0.24	0.80	-0.32	0.75	-0.29	0.90
	y	-0.89	1.00	-0.58	0.95	-0.48	0.75	-0.52	0.90
	z	-1.01	1.30	-1.00	1.55	-0.96	1.25	-0.92	1.70
XPOP	x	2.00	0.80	1.89	0.75	1.88	0.75	1.90	0.75
	y	-0.43	1.15	-0.03	1.15	0.08	1.15	-0.04	1.20
	z	-0.32	1.30	-0.49	1.75	-0.25	1.45	-0.34	1.50

* Acceleration values are in micro-g and data is being reported in the ISS-USOS Analysis Coordinates

Table 15. Ancillary Data for Data Sets and Increments Summary Tables

Ancillary Data		Increment-2			Increment-3			Increment-4	Increment 2/4
Attitude	Samples	Data subset 1	Data subset 2	Overall	Data subset 3	Data subset 4	Overall	Data Set #5	Overall
LVLH	Hours	508.0	0.0	508.0	198.3	769.4	967.7	1199.9	2722.1
	Points	114310	0	114310	44623	173117	217740	269974	612466
XPOP	Hours	341.8	8.0	349.8	2.0	647.7	649.7	1003.3	2002.8
	Points	76901	1802	78703	448	145724	146172	225750	450625

Table 16. 95th Percentile Histogram for all SAMS SEs for Increments 2 to 4

95%	Increment-2						Increment-3						Increment-4		
	Data subset 1			Data subset 2			Data subset 3			Data subset 4			Data set 5		
	Conditions (mg)			Conditions (mg)			Conditions (mg)			Conditions (mg)			Conditions (mg)		
	sleep	wake	both	sleep	wake	both	sleep	wake	both	sleep	wake	both	sleep	wake	both
F02		3.35	3.35				4.05	4.95	4.70	3.75	3.65	3.70	2.85	2.85	2.85
F03	2.20	2.15	2.18		2.48	2.48				1.60	1.65	1.63	1.95	1.98	1.95
F04	2.95	2.92	2.95							2.27	2.27	2.27	2.68	2.75	2.73
F05				0.14	0.24	0.22	0.25	0.30	0.28	0.24	0.27	0.26	0.20	0.28	0.26
F06	0.19	0.35	0.31	0.04	0.12	0.11	0.03	0.11	0.09	0.32	0.30	0.29	0.44	0.52	0.48

Table 17. 95th Percentile Histogram Results and Ancillary Data for Increments 2 to 4

95%				Increment-2			Increment-3			Increment-4			Increments-2/4		
	Ancillary data			Conditions (mg)			Conditions (mg)			Conditions (mg)			Conditions (mg)		
	freq	locat	Thrs	sleep	wake	both	sleep	wake	both	sleep	wake	both	sleep	wake	both
F02	200	ER-1	2853		3.35	3.35	3.75	3.65	3.70	2.85	2.85	2.85	3.20	3.15	3.15
F03	100	ER-2	2403	2.20	2.20	2.20	1.60	1.65	1.63	1.95	1.98	1.95	1.93	1.95	1.95
F04	100	ER-1	2269	2.95	2.92	2.95	2.27	2.27	2.27	2.68	2.75	2.73	2.63	2.70	2.68
F05	25	ER-2	2022	0.14	0.24	0.22	0.24	0.28	0.27	0.20	0.28	0.26	0.20	0.28	0.26
F06	25	ER-2	2862	0.16	0.29	0.25	0.28	0.27	0.25	0.44	0.52	0.48	0.38	0.45	0.41

Where: **freq**=frequency, in Hz; **locat**=facility to which sensor is attached to, and **Thrs** = total number of hours analyzed for each sensor for Increments 2 to 4, **ER**=EXPRESS Rack

Table 18a. 95th Percentile Results for Increment-2

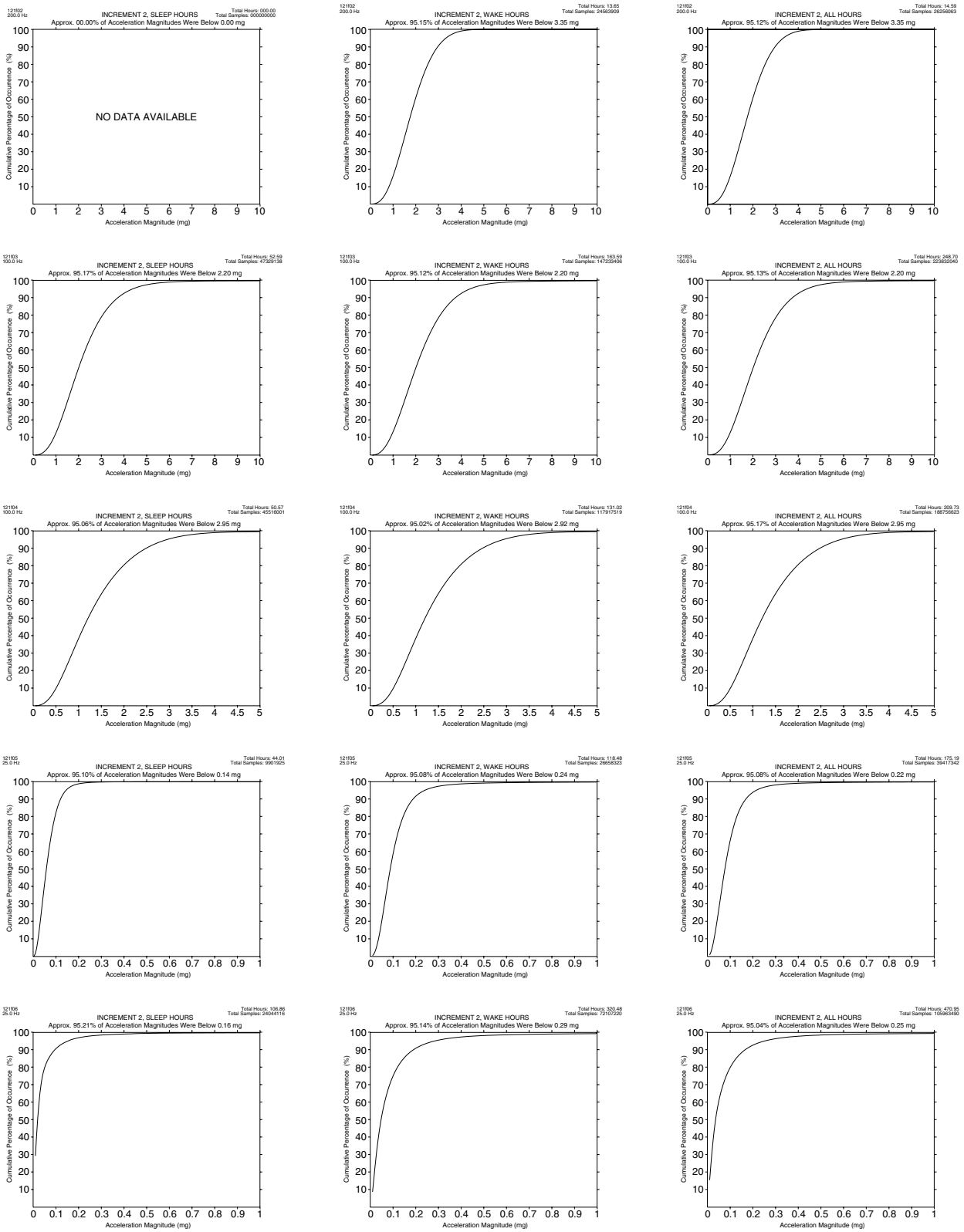

Table 18b. 95th Percentile Results for Increment-3

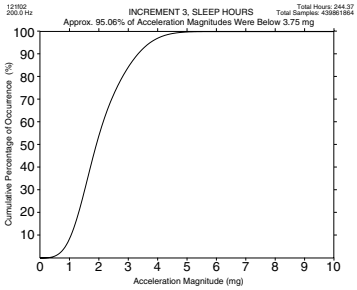

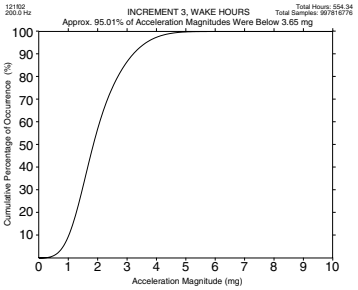

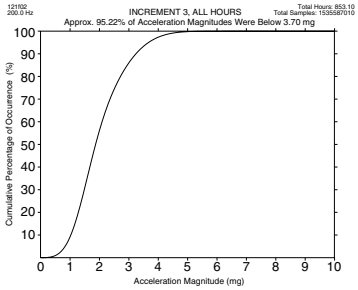

121F02

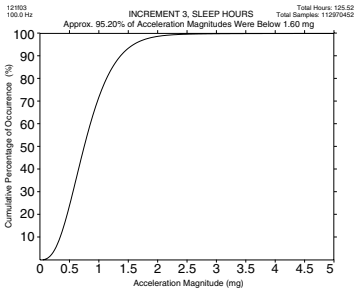

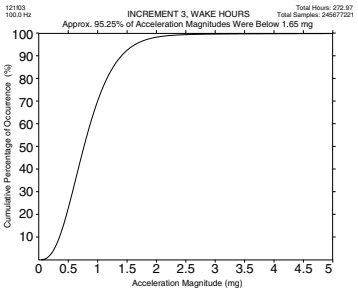

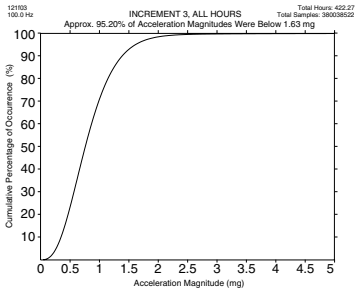

121F03

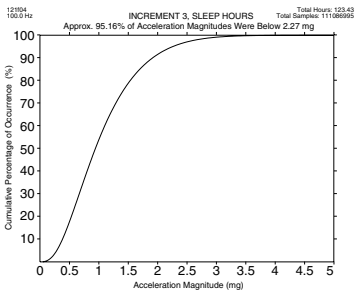

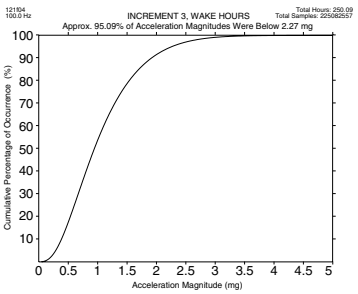

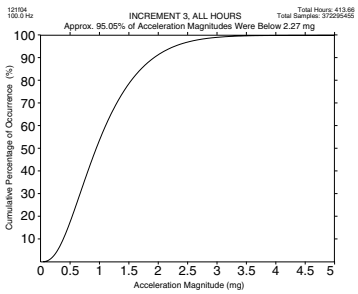

121F04

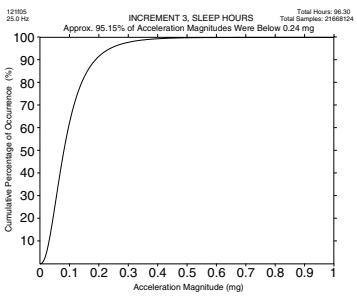

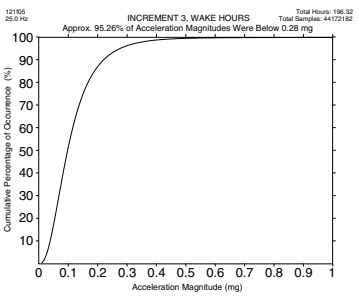

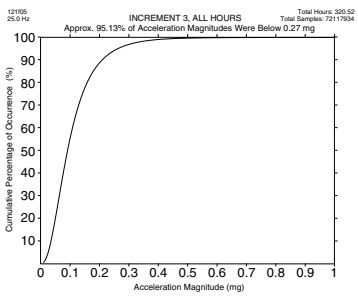

121F05

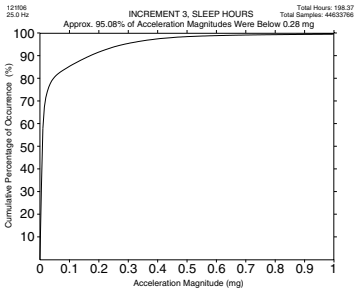

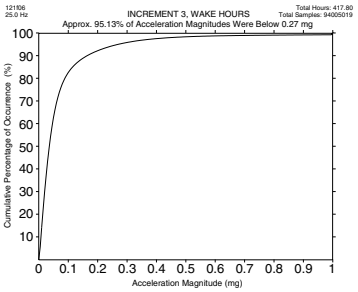

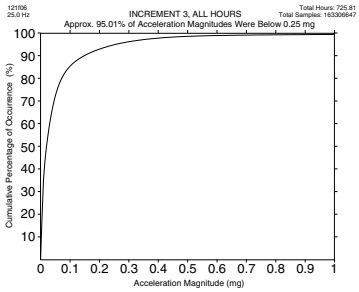

121F06

SLEEP WAKE BOTH

Table 18c. 95th Percentile Results for Increment-4

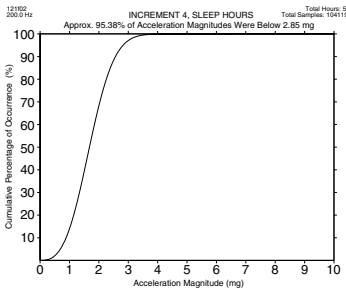

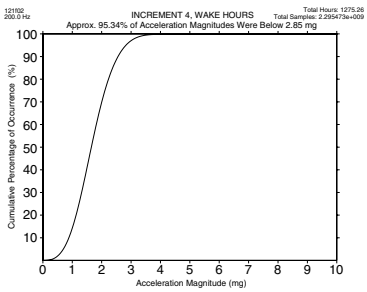

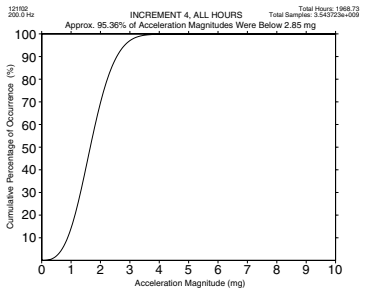

121F02

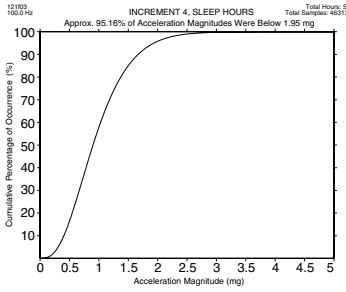

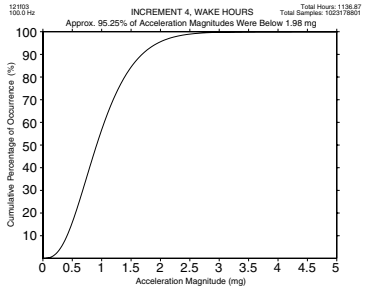

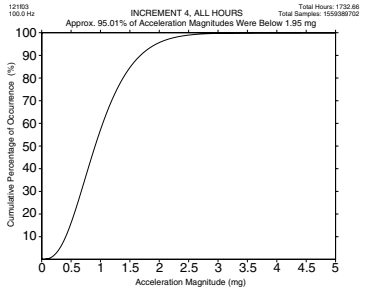

121F03

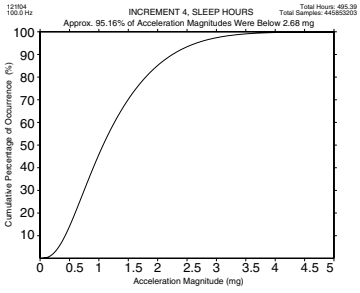

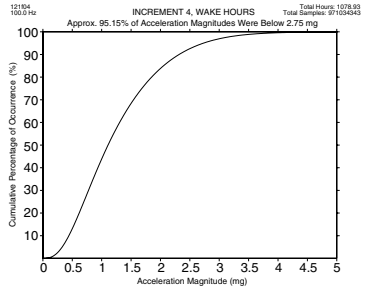

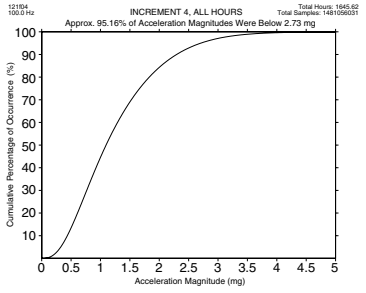

121F04

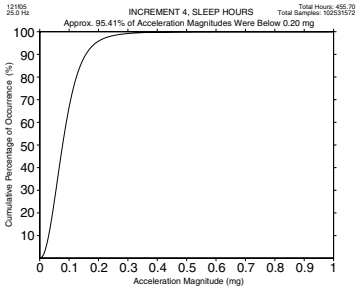

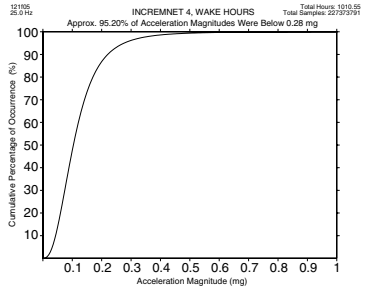

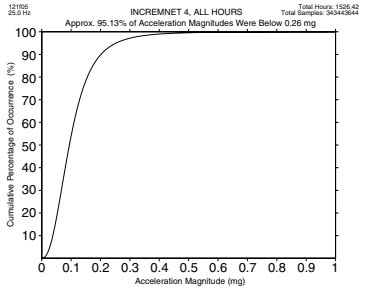

121F05

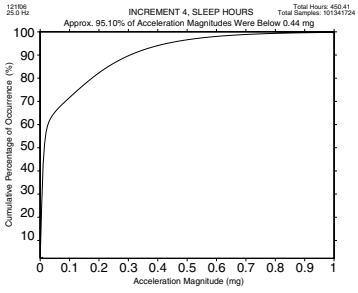

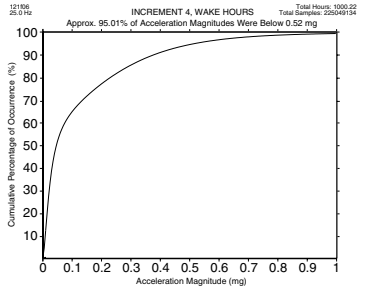

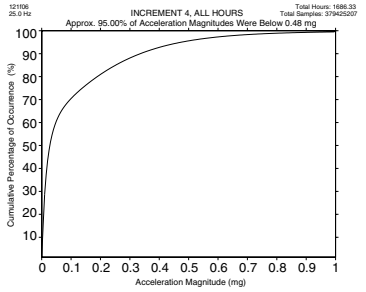

121F06

SLEEP WAKE BOTH

Table 18d. 95th Percentile Results for Increments 2 to 4

121F02

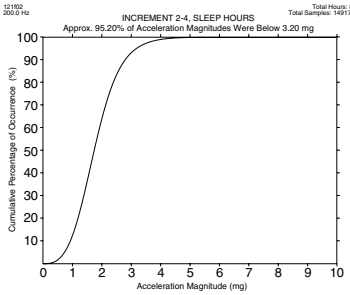

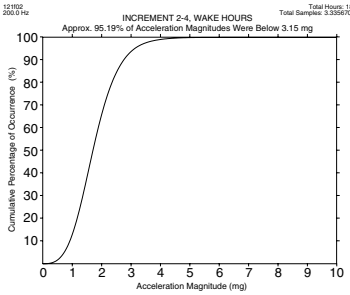

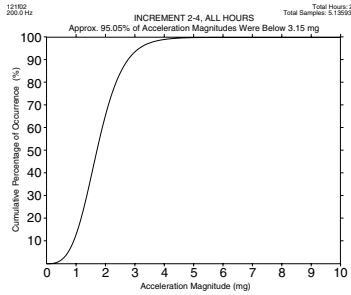

121F03

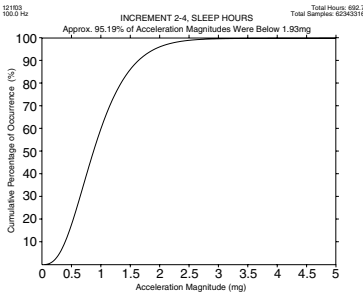

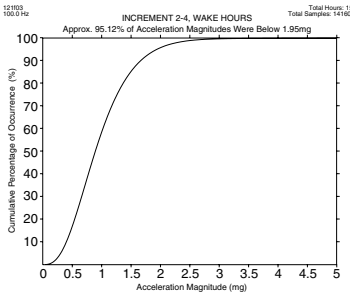

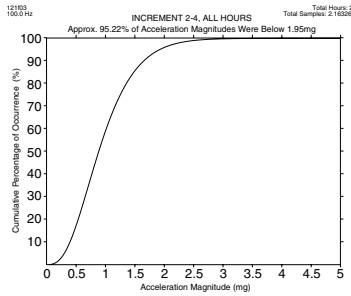

121F04

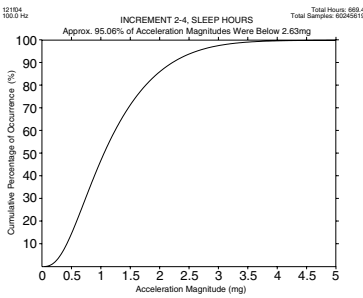

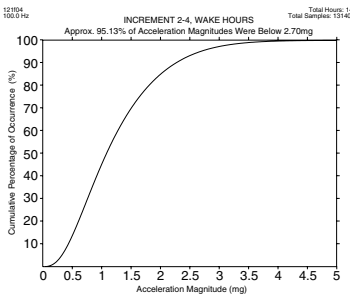

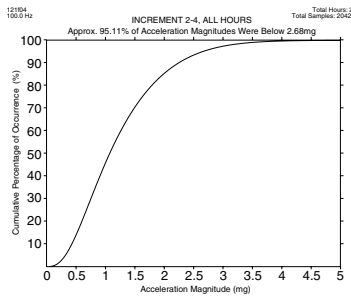

121F05

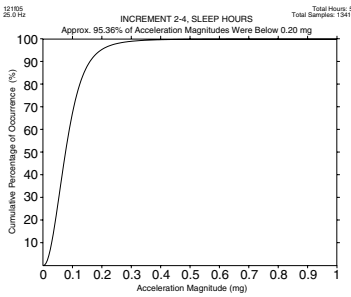

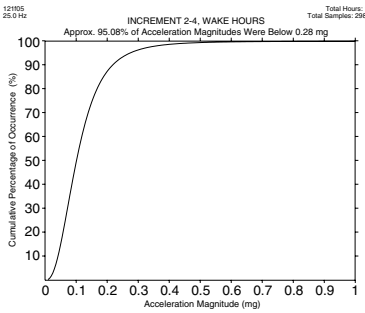

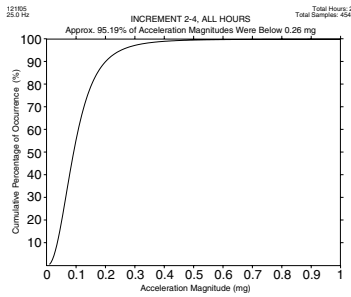

121F06

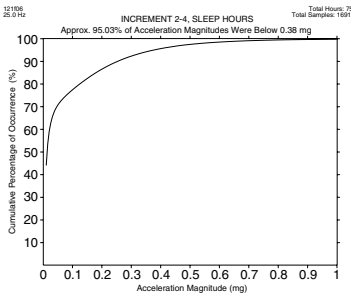

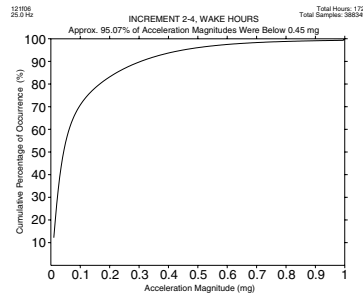

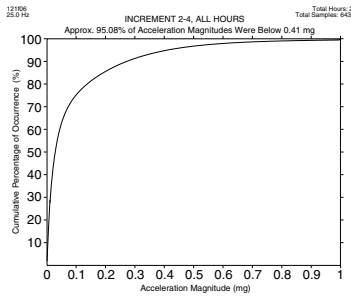

SLEEP WAKE BOTH

Table 19. 95th Percentile Results-- Comparison Between Filtered and Unfiltered Data for 121F03

121F03 (100 Hz)

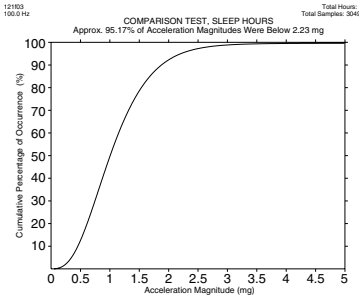

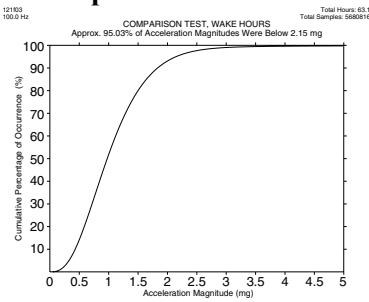

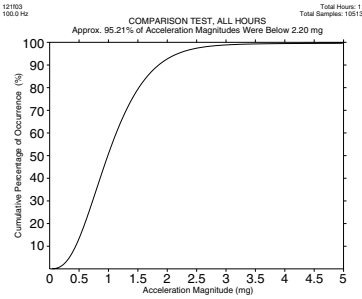

121F03 (5 Hz)

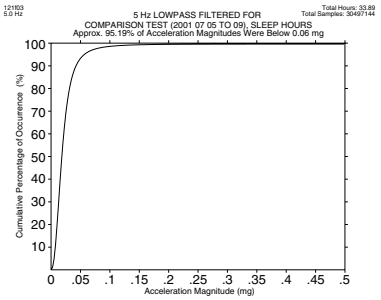

SLEEP

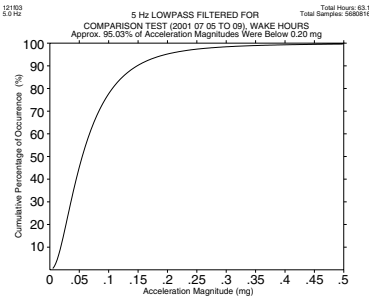

WAKE

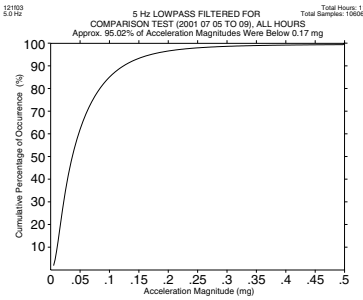

BOTH